PVT/PMT SYSTEM FEEDBACK DESIGN AND FEASIBILITY STUDY

A Thesis

by

RAINBOW YUHONG SUH

Submitted to the Office of Graduate and Professional Studies of
Texas A&M University
in partial fulfillment of the requirements for the degree of

MASTER OF SCIENCE

Chair of Committee,	Craig Marianno
Committee Members,	John Ford
	Yue Kuo
Head of Department,	Michael Nastasi

August 2020

Major Subject: Nuclear Engineering

ABSTRACT

Radiation portal monitors (RPMs) are employed worldwide at border crossings and other entry points as a method to detect the illegal transportation of radioactive material. Scintillating detectors composed of polyvinyl toluene (PVT) plastic are installed within the RPMs for vehicle and cargo screening, seeking gamma ray emissions that indicate the presence of radioactivity. A change in opacity referred to as fogging within PVT has been documented and is attributed to prolonged exposure in temperature and humidity fluctuations. The opacity changes lead to reduced light collection in the photomultiplier tube (PMT) and degradation in PVT over time due to irreparable microfractures. As part of an ongoing effort to combat PVT fogging, the purpose of this study was to develop a Opacity Monitoring System (OMS) capable of observing opacity changes in-situ. The OMS was tested, and the functionality demonstrated. The final design consisted of an array of multiple light emitting diodes (LEDs) as a light source, an optical sensor (OS), and a microcontroller board for data capture and transmission. The OMS was prototyped and tested at Texas A&M University for feasibility on small scale utilizing 0.038m x 0.152m x 0.762m (5 ⅞" x 3" x 1 ½") PVT samples, and full scale testing on 0.88m x 0.15m x 0.104m (2.9 ft x 0.5 ft x 0.125 ft) PVT panels in an environmental chamber at Oak Ridge National Laboratories. Light intensity data obtained through the OMS during testing was analyzed and showed clear indication of opacity changes in the PVT detector throughout multiple hours of extreme temperature cycling, thereby demonstrated the capabilities of the design and endurance of the hardware throughout extreme environmental changes.

DEDICATION

Dedicated to my brother Samuel Suh, who is first and foremost my friend.

ACKNOWLEDGEMENTS

I would like to thank my committee chair Dr. Marianno who gave an undergraduate a chance, and my committee members Dr. Ford and Dr. Kuo.

Thank you to Jeremy King, Ernesto Ordoñez, and my fellow colleagues.

CONTRIBUTORS AND FUNDING SOURCES

Contributors

This work was supervised by a thesis committee consisting of Professor Craig Marianno [advisor] and Professor John Ford of the Department of Nuclear Engineering and Professor Yue Kuo of the Department of Chemical Engineering.

All work conducted for the thesis was completed by the student independently.

Funding Sources

Graduate study was supported by a fellowship from Texas A&M University. Funding for this thesis research by given in part from the National Nuclear Security Administration/ Nuclear Smuggling Detection and Deterrence (NNSA/NSDD) program.

NOMENCLATURE

AMM	Absolute maximum to minimum
COTS	Commercial off the shelf
DLS	Digital light sensor
I^2C	Inter-integrated circuit
IDE	Integrated Development Environment
NORM	Naturally occurring radioactive material
OMS	Opacity Monitoring System
OR	Opacity ratio
ORNL	Oak Ridge National Laboratory
OS	Optical sensor
PVT	Polyvinyl toluene
PMT	Photomultiplier tube
RH	Relative humidity
RLM	Rise to local maximum
RT	Room temperature
RTC	Real time clock
RPM	Radiation portal monitor
SCL	Serial Clock Line
SD	Secure Digital
SDA	Serial Data Line

TABLE OF CONTENTS

Page

LIST OF FIGURES

Page

LIST OF TABLES

Page

CHAPTER I

INTRODUCTION

Timely detection of illicit trafficking to prevent improper use is a vital component of safeguarding nuclear materials. (Byers, 2013) Plastic scintillator detectors, particularly polyvinyl toluene (PVT), are widely deployed in radiation portal monitors (RPMs) due to the efficiency per unit cost compared to other detection materials and large detection surface area for vehicle screenings. (Kouzes, 2004) In the presence of gamma radiation, the fluorescent emitter suspended in the polymer base produces light, which is captured by a photomultiplier tube and transmitted as an electronic signal. RPMs must operate continuously and without failure regardless of the climate. Recently, a fogging phenomenon has been observed within PVT due to prolonged exposure to large temperature and humidity fluctuations between seasons. (Cameron, 2015) This phenomenon not only affects ongoing detection of nuclear materials, but also results in permanent damage to the plastic. Thus, the purpose of this research was to build and test a continuously operational monitoring system capable of detecting the onset fogging.

Degradation of polyvinyl toluene

Plastic Scintillator Detectors

PVT are plastic-based scintillating detectors capable of excitation by gamma ray interactions, which emit light through fluorescent molecules absorbing the excitation energy. The photomultiplier tube (PMT) detects the emitted light and converts light to electronic signals. (Lance, 2019) Within the last decade, abnormal behavior was observed in PVT-based RPMs where reduced scintillation light was collected through

the PMT over time. Routine inspection of the PVT eventually revealed the cause of such degradation to be linked to environmental fluctuations specifically in events of high humidity and low temperatures. The solution at the time required the detectors to be replaced well before significant degradation had occurred which results in a high cost burden. (Janos, 2019) These inspections and detector replacements also disrupted the flow of commerce; therefore, the goal was to determine the root cause and investigate possible technical solutions to extend PVT lifespan in the field. (Janos, 2019)

Characterizing Defects

The phenomenon known as fogging was characterized as a change in opacity within the body of the PVT after prolonged exposure to high relative humidity (RH) and temperatures that cycle between cooling and heating. (Lance M. J., 2019) The name refers to the appearance of a water vapor condensation similar to atmospheric fogging. Close inspection showed that the opaque appearance was caused by the presence of multiple disk-shaped defects. Some of the defects appeared to heal throughout the hydrothermal history of the plastic to the unaided eye, but larger magnification has proven this statement as false. (Lance M. J., 2019) (Cameron, 2015) Until recently, definitive proof for the root cause of PVT fogging had not been established and evidence remained circumstantial. (Janos, 2019) Recent studies have demonstrated that fogging and subsequent defects are the result of water particulate collection within the PVT polymer matrix which cause micro-fissure formations and degradations of the plastic from within. (Cameron, 2015) The fogging phenomenon was replicated in the laboratory setting through extreme temperature and humidity conditions to accelerate the effects.

Prolonged exposure to high heat allows water to consistently diffuse into the PVT at high RH. (Lance M. J., 2019) Thermodynamically, defect formation occurs when the water vapor clusters together in an effort to minimize contact from the hydrophobic plastic, the action of which morphs the polymer structure and causes densely packed crystalline regions. (Lance M. J., 2019) Increased tensile strain from the surrounding plastic compresses the water, effectively trapping moisture within the plastic. Freezing water has also been shown to aggravate defect growth. Liquid water is incompressible, which places further strain on the plastic when ambient temperatures drop below the freezing point. (Cameron, 2015) The expansion of water into ice state combined with the crystalline transformation of the plastic together cause cavitation within the disk shape defect, resulting in an overall fogging effect. (Lance M. J., 2019) The fogging has been shown to originate at the edges of the PVT plastic before diffusing into the center where it becomes fully opaque. Defogging likewise occurs in reversed order, becoming transparent beginning from the center of the plastic and growing toward the edges. (Sword, 2017) This change in opacity is retained until rising temperatures cause microfractures to expand and drive the water from within the plastic. However, the cavities created by the accumulation of water act as reservoirs within the plastic and have been shown to be the site of further water collection during the next temperature cycle. (Lance M. J., 2019) The growth of microfractures is highly aggravated by this routine, creating larger defects that also expand in diameter as temperatures continue to cycle. RPMs in some locations are regularly subjected to such cycling temperatures and humidity daily as well as seasonally. Defect formation during slow cooling are

exacerbated by the diffusion and coalescence of water in large isolated regions inside the plastic. Therefore, slow cooling has been shown to cause larger defects that are more visible after drying. (Lance M. J., 2019) Defect growth eventually lead to permanent degradation in the plastic over time.

Cameron estimates PVT lifetime to be approximately ten years in uncontrolled environments. (Cameron, 2015) Testing conducted by Sword at Oak Ridge National Laboratory showed that all PVT sustained permanent damage from environmental exposure through simulation in an environmental chamber. (Sword, 2017) Results from testing indicated that water could collect in the PVT plastic for long periods of time and remains undiscovered until the fogging phenomenon manifests due to cooling temperatures. (Sword, 2017) Lance postulated that defect growth is also accelerated by the aluminum RPM box that encases the PVT, which traps heat from the sun and increases the internal temperature by over 10°C. (Lance M. J., 2019) Therefore PVT defect is a serious issue for current RPM activities and operational sustainability in the long term. The time scale of fogging dissipation varied by detector slab size, where larger pieces of PVT plastic retained opacity longer than small sample slabs. (Janos, 2019) Thus, locations with annual environmental temperature swings and relatively high humidity were particularly concerning. With onset PVT fogging, changes in RPM efficiency are immediately seen. PVT loses light transmitting capabilities to the photomultiplier tube (PMT) as defects grow and decreases in the detector's functionality. Irreversible damage caused by the defects have been observed in detectors deployed worldwide. In order to maintain the required level of performance, additional

measures must be taken to either counteract or detect PVT fogging within RPM enclosures.

Currently, the onset of fogging remains virtually undetectable unless manual inspections of the detectors are conducted as defects may develop over several years. (Janos, 2019) Eventually, fogging becomes a permanent feature even at ambient temperatures and humidity as the buildup of micro-fissures grow within the detector. Some PVT fogging is acceptable within normal operational parameters. Adjustments such as detector recalibration can be conducted in response to any fogging discovered on inspection, however halting RPM operations for calibrations disrupts the flow of commerce. The portals must cease operations before an operator may open the enclosure to extract the PVT panels and remove the detector from its protective wrappings to determine the degree of fogging. Once removed from the wrappings, the detector is unusable and must be replaced. (Janos, 2019) Inspections that require substantial RPM downtime should therefore be minimized.

While some degree of transparency exists in the detector, the PVT may still be viable. An initial warning of onset of fogging is all that is necessary for operators to adjust procedure to compensate for changes in PVT capabilities. An indicator, proposed in this research, would allow operators to monitor fogging progressions and schedule maintenance and recalibrations only when necessary this would allow the RPMS to operate without limited interruptions. An in-situ indicator system capable of determining when opacity changes begin is the focus of this study and is one of the methods currently explored for mitigating PVT fogging effects during RPM operations.

Finding solutions to combat PVT degradation is still ongoing. The effort involved multiple approaches from discovering new material properties to constructing moisture-shielding devices. Currently, manufacturer Eljen Technology has fielded new fogging-resistant plastic detectors. (Janos, 2019) Predictive modeling to plot the time evolution of water within plastic detectors through existing temperature and humidity histories has also been produced. (Payne, 2019) Aside from combating degradation, the development of an In-situ monitoring system was determined to be one of the most effective and immediate solutions to combat PVT degradation. Until a final solution may be established to prevent fogging in plastic detectors, the feedback system from this study will likely be integrated into RPMs to alert operators of opacity changes. Even after a permanent solution to fogging is found, the feedback system can remain as a watchdog. Design of the proposed opacity monitoring system for RPMs must therefore consider some physical and operational parameters, including size restrictions to the hardware design, uninterrupted signals from detector, low overall manufacturing cost, and replicable.

CHAPTER II

CONCEPTUALIZATION

Opacity Monitoring System

Design Considerations and Objectives

This study concluded with the design and testing of a feedback system capable of tracking PVT degradation over time by observing opacity change and is known as an Opacity Monitoring System (OMS). The design must be easily integrated into existing RPM systems and not interfere with regular portal operations. Therefore, some restrictions and design criteria were considered. The OMS must be confined to the limited available space inside an RPM enclosure, which dictated the size restrictions for all hardware components. The system must also be robust and withstand environments where RPMs are deployed. OMS data must clearly indicate a change in opacity, and the format must be easily integrated into the existing data stream sent from the portal monitors. As there are many RPMs operating worldwide, the final design and construction of the OMS must be easily replicated and at low cost.

Light Intensity Method

Considering the design objectives and restrictions, it was determined that measurements of light intensity would be the OMS's fundamental method of opacity monitoring. Opacity is the degree of visibility from one side to the reverse and often used to characterize the optical properties, density, or mass concentration of specific materials. (Science Direct, n.d.) An optical sensor for gauging the amount of captured light placed opposite a steady light source would measure the increase or decrease in

brightness. If the material between the sensor and light source was to change in opacity, a change in the brightness will be perceived by the sensor. Theoretically, the change in brightness is proportional to the opacity change. It was known that PVT free of fogging is transparent and would grow opaque in a steady manner, therefore any light that passed through the detector will become slowly obstructed. Thus, any increase or decrease in light intensity measured continuously would indicate a change in PVT opacity. Conventional opacity meters exist in various field applications such as the glass industry or plastic fiber industry and are also based on the principle of a photo-diode and a constant light source. (Singh, 2010)

Utilizing light to measure opacity is a common method across various fields of study. Opacity monitoring is commonly used to measure gaseous emission in air and pollution density in water. One such method for assessing smoke density known as The Ringelmann Smoke Chart based on the Ringelmann method that characterized the density of smoke by visibility. (Stuart, 2017) Other applications of light intensity method include forward-scattering laser measurements of particulate matter to enhance optical clarity of instruments in dense particulate environments. (Fry, 1992) The theoretical method of light intensity measurements met all this project's critical objectives and stayed within the design restrictions. The hardware required to execute the method, the construction, and the testing are discussed.

Hardware and Software

LED Light Source

As the main light source in the OMS design, light emitting diodes (LEDs) were chosen based on durability and replicability. LEDs were commercially available, reliable, and easily integrated into the design.

Table 1. LED brightness and wavelength by color reported by manufacturer Adafruit Industries.

LED	Brightness (lux)	Wavelength (nm)
Red	1500	630
Yellow	1800	590
Blue	6000	465
Green	8000	525
White	15000 (minimum)	

A variety of LED colors were involved in the initial design and testing of the OMS to investigate possible effects of LED brightness on the design. From Table 1, the LEDs vary in brightness with the red LED reporting lowest light intensity and the white LED reporting the highest light intensity. A variety of LED colors were tested that spanned the visible wavelength spectrum. All LEDs are 5 mm super bright LEDs composed of indium gallium nitride (InGaN). The operating voltage was 3V with 20 mA absolute maximum rated current. The brightness was rated at standard room temperature of 25 ºC. The units associated with illuminance are lux or one lumen per square meter. The super bright LEDs were chosen for the design to ensure as much light passed

through the detector face as possible. Step changes in light intensity within PVT was predicted to be best visualized if the light source was as bright as possible. For voltage regulation, a 10 Ω resistor was soldered to each LED. Figure 1 shows the LED as prepared for testing with the resistor and heat shrink wrap. The heat shrink ensures the solder joint between LED and wire was protected from environmental factors and provided a clean finish to the construction.

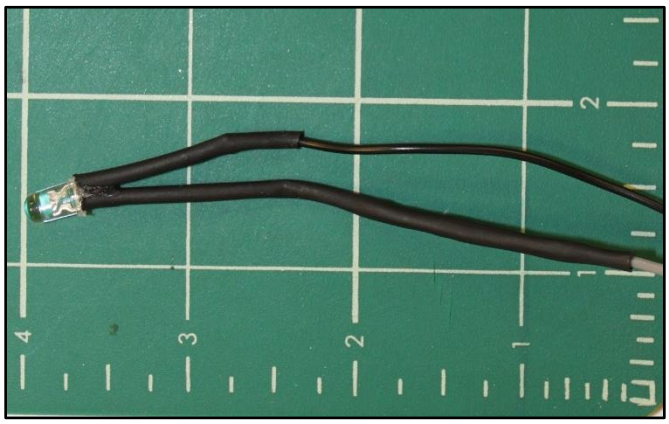

Figure 1. An LED soldered with a 10 Ω resistor as prepared for testing with heat shrink wrap.

Microcontroller Including Data Logger Sahield

Power and data logging capabilities of the OMS relied on an integrated circuit known as a microcontroller. The parameters of the OMS required well-documented or open source hardware that was both highly functional and commercially available. The Arduino Mega 2560 microcontroller board fulfilled both criteria and was therefore selected for the OMS hardware design. Based on the ATmega2560 microcontroller, the Mega 2560 board included 54 input/output pins, 16 MHz crystal oscillator, USB connection, power jack, and a reset button, all in support of the microcontroller.

Capabilities of the microcontroller could also be expanded through shield designs available such as data logging with a SD (secure digital) shield. The Adafruit Data Logger Shield was integrated into the OMS build to increase microcontroller's data storage capabilities. Similar to other components of the OMS, the SD shield was well supported with online documentation and libraries made available through Adafruit and Arduino. Integrating the SD shield into the functionality of the microcontroller was simple and straightforward. The SD shield is compatible with standard formats of commercial SD cards and is capable of reading and writing data quickly with a 3.3 V level shifter. (Adafruit, 2013) As measurements are taken by the lux sensor, a copy of all data is stored locally and simultaneously read through the computer terminal. The shield included a real time clock (RTC) component that allowed timestamps to be included in the serial data stream.

Optical Sensor

To register light transmission an Adafruit Industries TSL2561 Digital Light Sensor (DLS) breakout board consisting of a Texas Advanced Optoelectronic Solutions optical sensor (OS) was used. The TSL2561 was chosen based on its precise light detection capabilities, with ranges from 0.1 to 40,000 or more lux. (Adafruit Industries, n.d.) The lux sensor meets the low cost and replicability requirements of the design requirements.

The TSL2561 was a well-documented piece of hardware and has a worldwide user-base. The sensor also utilized built-in analog-digital converters which allowed for use on any microcontroller board even if analog inputs were unavailable. (Adafruit

Industries, n.d.) Overall current draw for the sensor was low, at less than 15 µA when in power-down state and 0.5 mA when actively sensing, and thus suitable for the low power data-logging design of the OMS. Combined with the LEDs, the lux sensor completed the hardware requirements to implement the method of light intensity measurement. Utilizing the inter-integrated (I^2C) communication protocol, light intensity converted to digital signal output by the OS would be transmitted to the microcontroller. (TAOS, 2018)

Construction

The OMS was constructed at Texas A&M University using the previously specified hardware. A summary of the components can be found in Table 2 and the final circuit diagram can be found in Figure 2. The microcontroller and OS utilized I^2C communications, where the Serial Clock Line (SCL) and Serial Data Line (SDA) are the required lines for a master and slave computer to send and receive data. As a non-computing component, the LED only required a digital pin port for power transmission that simultaneously regulated the brightness. To facilitate testing, wiring was not directly soldered to the OS board, but rather a stacking header was used that would sit flush with the board pins.

Table 2. Summary of the OMS hardware components, corresponding pin onboard the Arduino Mega 2560 microcontroller, and the associated colored wire.

Component	Wire Color	Arduino Pin
OS SCL	Green	SCL
OS SDA	Blue	SDA
OS Voltage In (Vin)	Red	5 V
OS Ground (GND)	Black	Ground
LED Positive (+) Wire	Gray	Digital Pin
LED Negative (-) Wire	Black	Ground

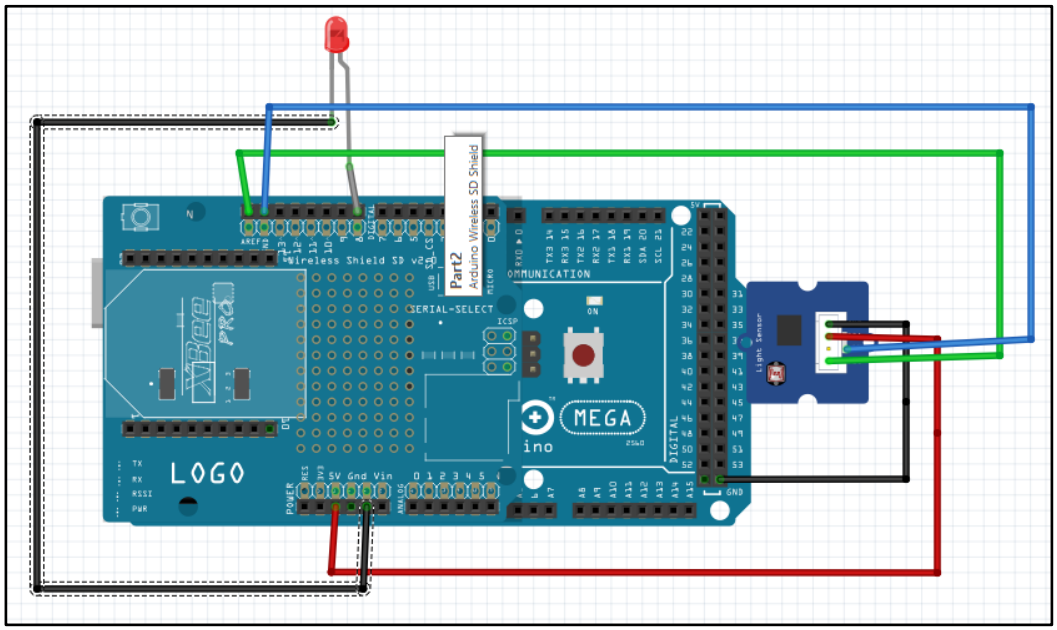

Figure 2. Representation of the OMS components attached to the associated ports onboard the Arduino Mega 2560 microcontroller.

Figure 3. The TSL-2561 digital lux sensor with the stacking header that attaches to the respective pins on the OS board.

Assembly of the lux sensor was conducted as follows. Electrical wires were soldered to a stacking header that matched the pins of each component. This was to prevent prolonged contact between the components and high heat which may jeopardize the integrity of the hardware. All soldered joints were sealed with a commercially available heat shrink wrap that minimized contacts between neighboring joints and offered some barrier between the exposed components and the environment (as seen with the LED configuration in Figure 1). The heat-shrink wrap also encloses additional pieces such as the 10Ω resistor.

Data Acquisition

Data capture and overall function of the OMS was developed in Arduino's integrated development environment (IDE) and written in the Arduino language, composed of C and C++ functions (Arduino, 2015). The procedure executed by the Arduino Mega microcontroller was as follows. LEDs emitted light and a 1 ms delay occurred before the lux sensor recorded light intensity. The integrated delay ensured the LED would reach maximum brightness prior to the measurement. In total, light emission from each LED lasted 1 s. Recordings from the lux sensor was transmitted in serial format from the computer through the SD shield and logged via the open-source application CoolTerm. (Meier, 2018) Through CoolTerm, the data output was read during and after testing. The procedure repeated in 60-s intervals until the program was terminated by either manually stopping the script through the computer or through a loss of power. Digital data collected throughout testing was copied and stored on a SD card mounted on the Arduino SD shield. The serial data stream output included a timestamp in seconds starting with 0 s at the beginning of each run session and a lux value. The two values were distinguished by a separating comma. Serial data could then be integrated into a spreadsheet program such as Microsoft Excel for analysis.

CHAPTER III

PROTOTYPE DESIGN

Design Verification

Laboratory Prototype Testing

The OMS prototype was constructed and tested to verify its functionality. The tested prototype setup included a single white LED and an OMS detailed in Figure 4. The LED and OS were mounted to opposing faces of a 14.92 cm x 7.62 cm x 3.81 cm samples of PVT with electrical tape. To simulate the setting within an RPM enclosure, the PVT detector and attached OMS components were wrapped in a layer of commercial aluminum foil followed by a layer of electrical tape analogous to standard PVT wrapping techniques developed by the detector manufacturer, Eljen Technology. Wires extending from the wrapped detectors were secured with electrical tape to ensure a tight seal against moisture and light leakage. Double layers of electrical tape were placed where the wires protruded, which can be seen in Figure 5. Three PVT samples-OMS systems were prepared in this manner for fogging and system design testing. In total, four 14.92 cm x 7.62 cm x 3.81 cm sized PVT detectors were used throughout the prototyping stage. Three PVT detectors of the size were prepared in the manner described, but with different colored LEDs in each OMS. The wrappings were only removed in the event of troubleshooting or to change LED colors. The fourth PVT detector of size 14.92 cm x 7.62 cm x 3.81 cm was devoid of OMS and wrapping which

served as a visual indicator of whether opacity changes were occurring to the wrapped detectors without unwrapping them for inspection.

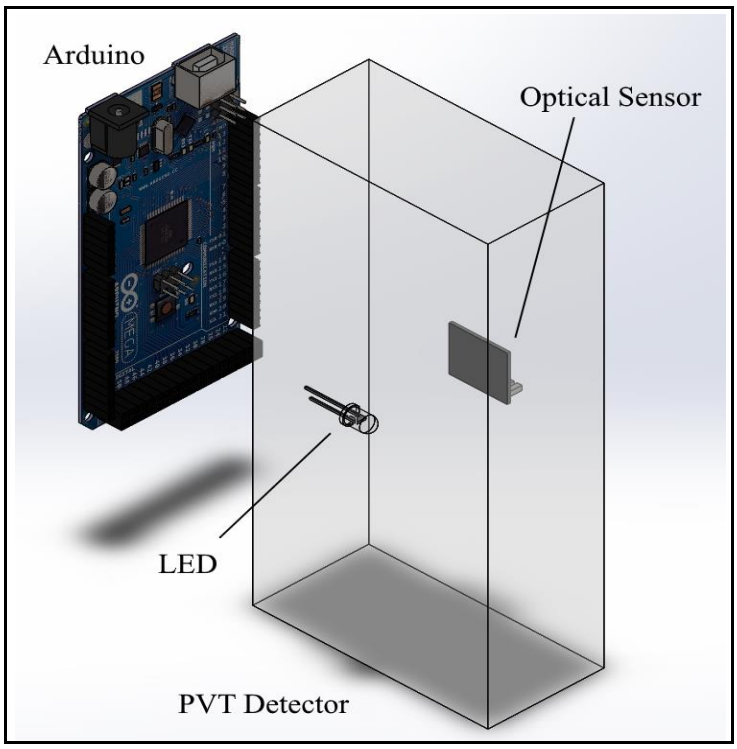

Figure 4. Prototype OMS side view mounted on a 14.92 cm x 7.62 cm x 3.81 cm PVT detector showing orientation of the LED and OS across parallel planes of the detector.

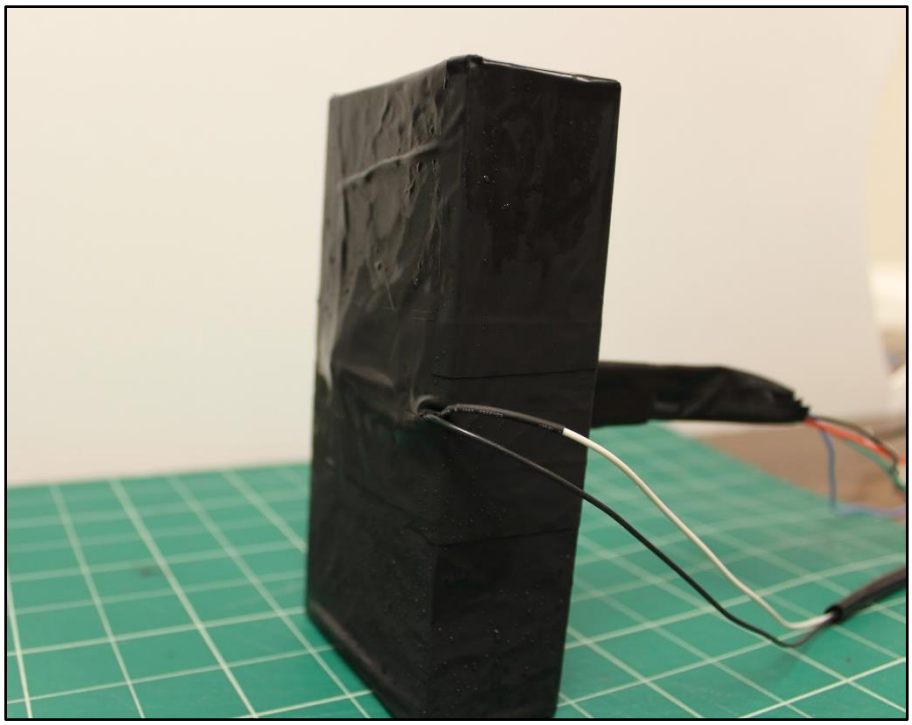

Figure 5. A PVT detector and OMS wrapped in aluminum foil followed by electrical tape. Wiring for the OMS protrudes from the wrappings leading to the microcontroller (not shown).

To induce detector fogging, a high humidity and high temperature environment was required. A laboratory designed environmental chamber was built comprised of a 71 L ice chest, an infrared livestock heat lamp, an Inkbird ITC-308 outlet thermostat temperature controller, and a pan of water. Due to the size of the small-scale testing, an ad hoc environmental chamber was enough to produce the high temperature and high humidity conditions. A designated laboratory environmental chamber ensured constant access and simulated the required high temperature and high humidity environment at all times. Acquiring a full-sized environmental chamber for testing was challenging, therefore a small in-house setting was more appropriate for prototyping purposes. It

should be noted that further testing beyond prototyping requires the full scale 3.8 cm x 15.2 cm x 76.2 cm PVT detectors, which was too large for the demonstrated environmental chamber. Full scale testing will be discussed. In the prototyping stage, a remote humidity sensor was initially included in the environmental chamber design however sensor readings were unreliable and was removed.

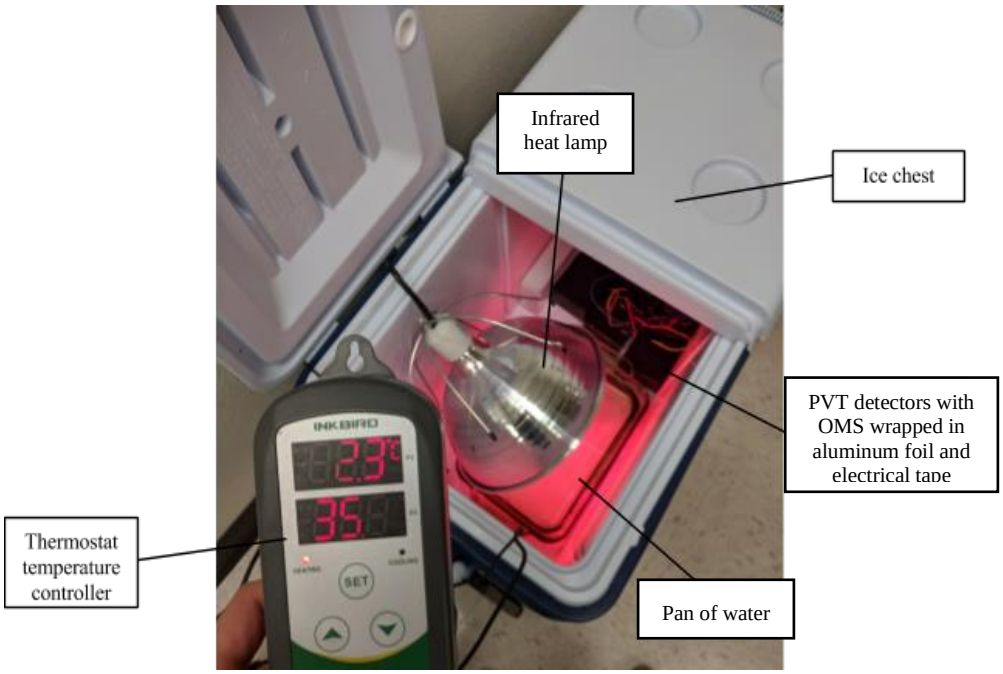

Figure 6. The laboratory designed environmental chamber including infrared heat lamp, water source, thermostat temperature regulator, and wrapped PVT detectors.

The ice chest created an insulating container which allowed a heat lamp and a small volume of water at the bottom to generate a humid environment. The heat lamp was connected to the thermostat temperature controller which maintained the internal temperature within the ice chest at 45 ± 2 °C by actuating power to the heat lamp intermittently. The bare detector and three wrapped detectors were placed inside ice chest environmental chamber suspended two inches above the ice chest floor with a wire

rack to prevent the detectors from soaking in accumulating water. The laboratory environmental chamber can be seen in Figure 6. In total the detectors were exposed to the high humidity and high temperature environment for seven days (168 hours). This was to ensure complete water penetration into the plastic scintillator until the saturation point was reached. The soaking period was immediately followed by 24 hours of freezing -7 ± 1°C at relative humidity (RH) in a commercial chest freezer. The trapped water inside the PVT subsequently induced the fogging phenomenon.

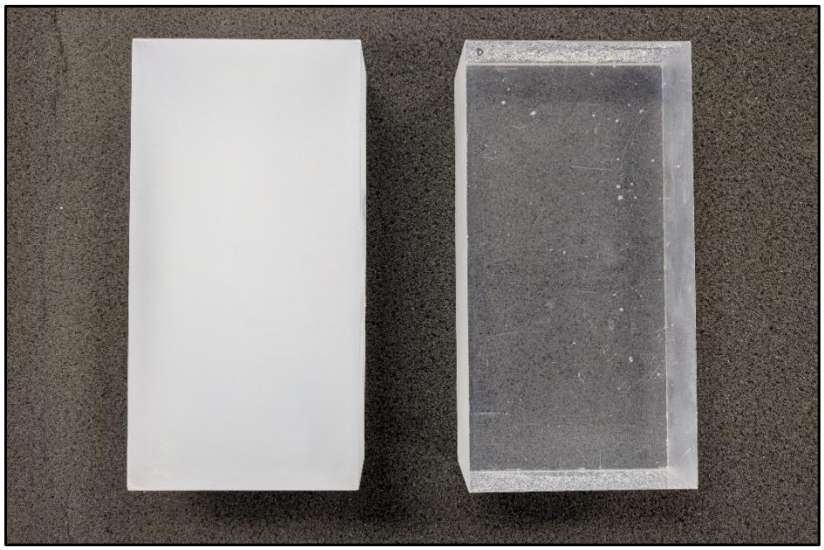

Figure 7. Two PVT detectors of size 14.92 cm x 7.62 cm x 3.81 cm, one fully opaque from high temperature and high humidity soak and 24 hours of low temperature and RH (left), and the other transparent at RT and RH (right).

Opacity change was successfully achieved in the simple environmental chamber. Figure 7 compares a PVT detector following 168 hours of soaking and 24 hours of freezing next to an un-soaked and un-frozen detector. Some defogging was observed in the detectors when freezing periods were prolonged, possibly due to water sublimation

action out of the plastic. Therefore, the wrapped PVT were kept in the freezer for a maximum of 30 hours following the 24-hour freezing period. Though data acquisitions were conducted with a single detector at a time, multiple detector/OMS systems were soaked and frozen simultaneously to minimize waiting time between testing sessions. Soaked detectors were stored in the freezer before testing to ensure maximum fogging within the PVT at the beginning of each data acquisition session.

Data Acquisition Testing

Prior to soaking and freezing session, light intensity measurements were acquired using the OMS while the detector was still transparent. These values are considered the 'baseline' and were used for comparison purposes when analyzing the light intensity measurements taken during and after PVT recovery. The light intensity values were expected to remain steady and unchanging for multiple hours because the environment surrounding the PVT is unchanging and likewise the detector should not change in opacity. Likewise, upon PVT recovery from fogging, the light intensity was expected to read similarly to the baseline values, indicating the PVT had reverted to full transparency. The baseline values were recorded using red, green, blue, and white LEDs. Data acquisition sessions began immediately after the soaked and frozen PVT detectors were removed from the freezer. Data capture was conducted on one PVT/OMS at a time. A frozen detector was placed inside a light-minimizing protective case to simulate the low light environment of an RPM enclosure but also to minimize possible light interference to the OMS at the start of each testing session. The OMS was wired to the appropriate pins of the Arduino Mega microcontroller which was also placed inside the

protective case to minimize wire length. Power was provided to the microcontroller by USB cable from the designated testing computer, which also transmitted data between the microcontroller and computer. Illustration of the OMS data acquisition environment can be seen in Figure 8 with the testing computer sitting on top of the protective case containing the fogged detectors.

As the temperature of the wrapped PVT detector increased from freezing, trapped moisture would evacuate the plastic scintillator, causing a return to transparency at room temperature (RT) and RH. This sequence of events was referred to as PVT recovery. CoolTerm transmitted OMS lux data, and the progress of the PVT recovery was monitored. A copy of the serial data was written to the computer as well as an SD card on the Data Logger Shield on board the Arduino Mega. The data capture sequence was monitored until a distinct plateau in lux reading was achieved. This was the indicator that the detector had reached maximum transparency, as the readings of transmitted light stabilized between captures. Various data acquisition tests conducted with the three wrapped PVT detectors all varied in recovery time from 25 to 35 hours of total capture time.

Figure 8. Arrangement of the OMS data acquisition testing environment showing the protective case containing the PVT detectors with onboard OMS and Arduino Mega microcontroller (unseen), and the testing laptop with USB running between computer and microcontroller.

Data from otype Testing

From the results of the laboratory test, the prototype OMS proved successful. The combination of LED and lux sensor could indicate opacity change within the wrapped PVT detector through a series of light intensity measurements. Opacity changes were also trackable in small increments over time which allowed for the visualization of PVT opacity changes. The robust COTS hardware of the OMS was still operational after multiple environmental changes; however, some component failures did occur.

These component failures occurred in such incidents as shifting or transporting of the PVT and OMS between locations. Transportation was the known cause of these

failures as tests prior to transport would indicate a working OMS, but then fail to function properly after moving. Shorts also occurred in the wiring as the LEDs would suddenly extinguish after a few hours of tests or fail to start completely. This may be due to water uptake into the wrapped PVT detectors and into the LED wiring or poor wire connections. Loose soldering joints that broke off during testing or failed to transmit power entirely was another point of failure. Many of the issues were resolved by re-soldering and wiring of LEDs with new sturdier wires and sealing each end of the shrink-wrap with E6000, a water-resistant commercial adhesive. The lux sensor and microcontroller both maintained functionality and suffered no failures throughout the prototyping stages, though some soldering joints on the stacking header came loose and required re-soldering and reinforcing with shrink-wrap and E6000.

Baseline Light Data

Results from the baseline measurements tests also served as initial gauges for the data acquisition system. Initial baseline measurements were taken with blue LEDs for eight hours and with green LEDs for six hours. Steady levels of light intensity were seen, such that a consistent lux value was maintained and only small fluctuations between one to five lux was observed. This steady state was expected given the un-fogged state of the PVT detectors at a constant temperature and RH. Subsequent baseline measurements with red LEDs and white LEDs were taken over a shorter period as the steady state was demonstrated by the blue and green LEDs prior, and the testing procedure needed to continue to the data capture portion. OMS data acquired during PVT recovery was compared to baseline measurements as a function of LED color.

Unexpected features were revealed when inspecting the baseline data and is discussed as follows. From the green LED, baseline light measurements averaged at 920 ± 5 lux over the course of eight hours. Light intensity from the green LED during PVT defogging was measured over the course of 16.2 hours and was shown to increase asymptotically from a minimum of 467 lux to 828 ± 2 lux. Measured light from the green LED did not recover to the brightness of the baseline measurements.

Light from the blue LED showed a gradual decrease over the 8-hour duration of the baseline measurements. The initial light intensity value was 2110 lux and the final stable value was 2081 lux, with an average intensity was 2098 ± 13 lux. All data fell within 2σ of the average value for the blue LED. The recovery test was over the course of 12.8 hours before data acquisition was concluded. Light intensity from the blue LED did not reach a steady state and was predicted to continue increase beyond the average baseline light intensity, therefore acquisition was concluded. Over the duration of 12.8 hours, the light intensity from the blue LED increased asymptotically throughout PVT recovery from a minimum of 990 lux to 2076 ± 1 lux and was still within 2σ of the baseline average.

PVT Recovery Light Data

Multiple data acquisitions sessions with PVT recovery were conducted and it was shown that each LED exhibited differing behavior. Summary of the values are found in Figure 9. A comparison of blue, red, green, and white LED data showed similar features across time and intensity. All light intensities began at a low lux value, synonymous with an opaque PVT detector. The measured light then increased asymptotically over time as

the PVT detector defogged and reached a maximum lux value as the detector approached transparency. The maximum value then stabilized for the remainder of the acquisition time resulting in a plateau of light intensity.

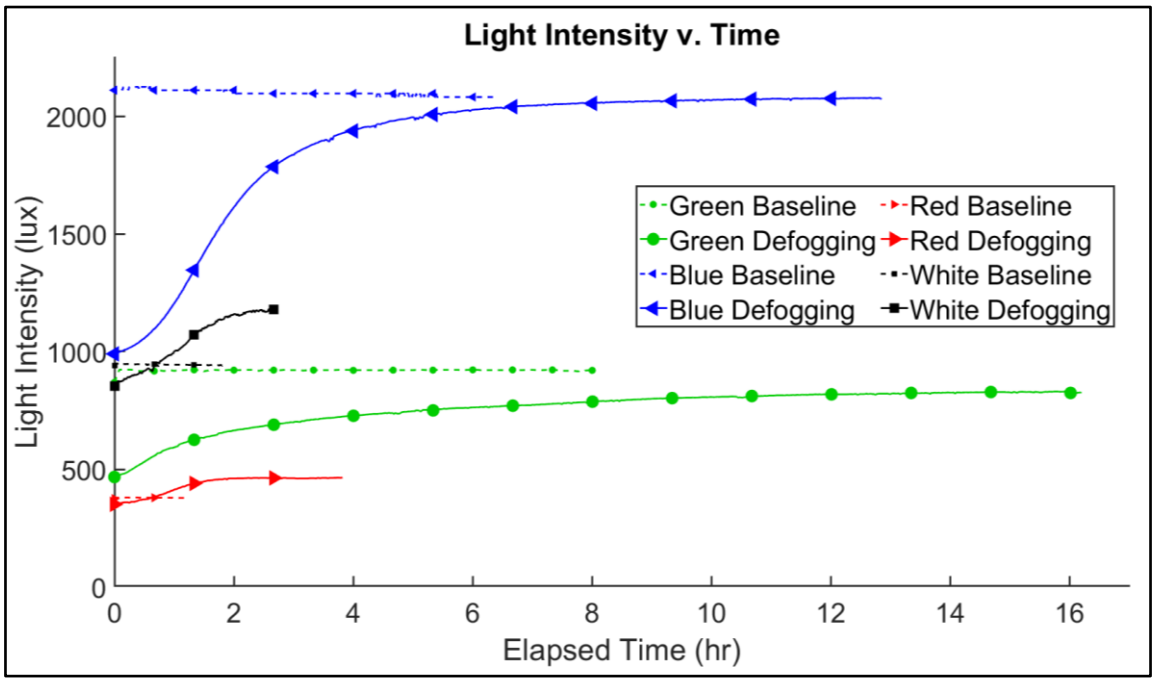

Figure 9. Comparison of light intensity data acquired at full PVT transparency (baseline) and during PVT fogging recovery.

The green LED reached a plateau in light intensity over the longest period of time as seen in Figure 10. In total, the measured light range was 361 lux from the minimum lux and maximum lux. However, measured light at full transparency failed to correspond with the baseline light intensity. The average light measured for the baseline was 920 ± 5 lux, while the light intensity averaged throughout PVT recovery was 828 ± 2 lux. In total, the light measured from the green LED following PVT recovery deviated

from the baseline measurements taken prior to PVT fogging. The deviation was 92 ± 5.4 lux which equates to a percent difference of 10%.

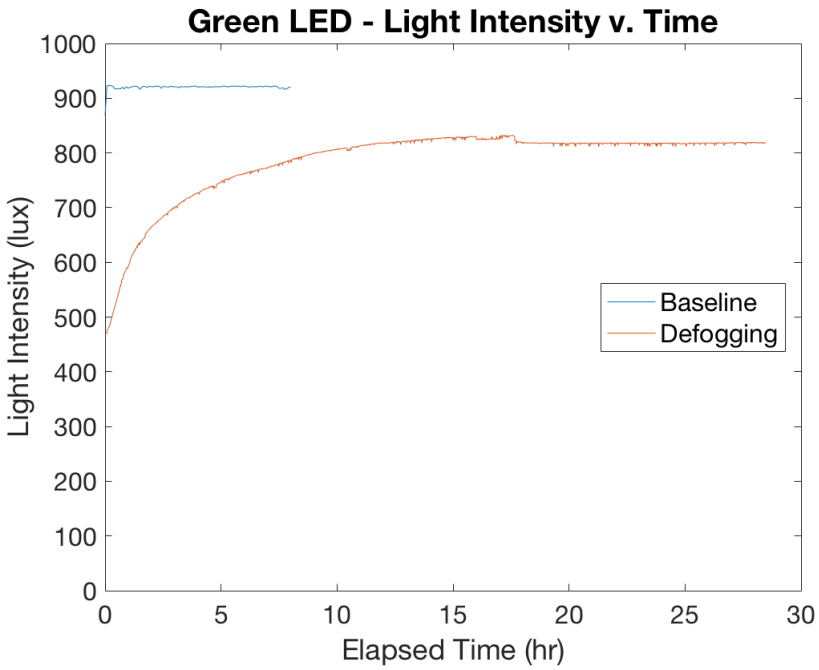

Figure 10. Light intensity from OMS testing with green LED. Light intensity increased asymptotically to a plateau below the baseline intensity measurements.

Light from the blue LED plateaued at a faster rate than the green LED during PVT recovery, seen in Figure 11. Blue LED light measurements also possessed the greatest range, 1086 lux, between the minimum and maximum light measured. The light approached the initial baseline value in an asymptotic manner and reached a steady state within 2σ of the baseline average, despite the blue LED baseline measurements showing a slight decrease in lux over time. The baseline light intensity averaged 2098 ± 13 lux while the measured light at PVT recovery averaged 2076 ± 1 lux for a total percent difference of 1% between the values.

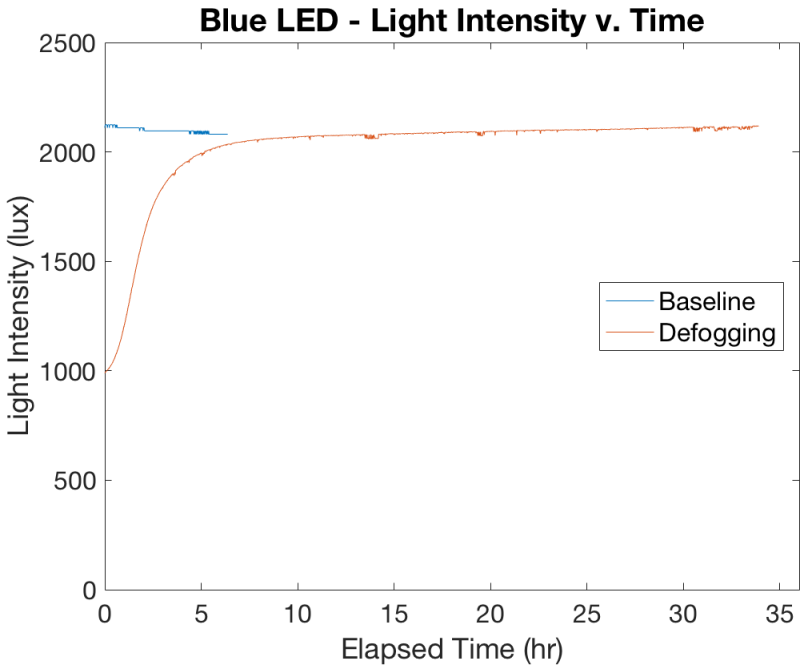

Figure 11. Light intensity from OMS testing with blue LED. Light intensity increased asymptotically to a plateau near the baseline intensity measurements.

As previously mentioned, consecutive failures involving the OMS with the white LED terminated further prototype testing. Two examples of such failures can be seen in Figure 12 and Figure 13. Figure 12 shows an instance of failure where wiring problems resulted in the lux sensor reading default values of 65550 lux. Attempts to resolve the issues were made including reinforcing soldering joints, addition of sealants to all wiring ends to prevent water uptake and exchanging OMS components. Some functionality was restored, but other failures occurred such as seen in Figure 13 where acquisiton ceased mid-test and no error values were shown by the OMS. Expected error values included 0.0 lux which indicates no light emission from the LED or high 65550 lux, the default lux readings, indicating lux sensor is active but not functioning properly.

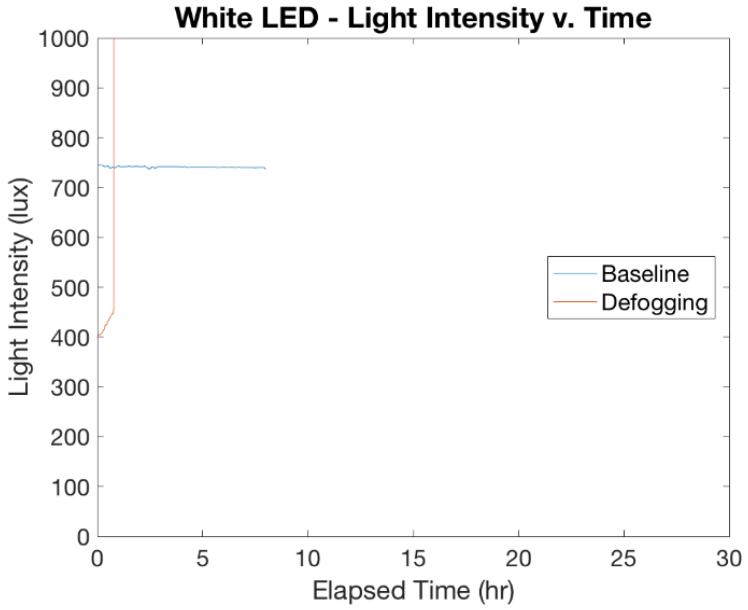

Figure 12. A sample case of OMS testing with white LED leading to hardware failure, where unknown wiring failure resulted in the lux sensor reading default lux values.

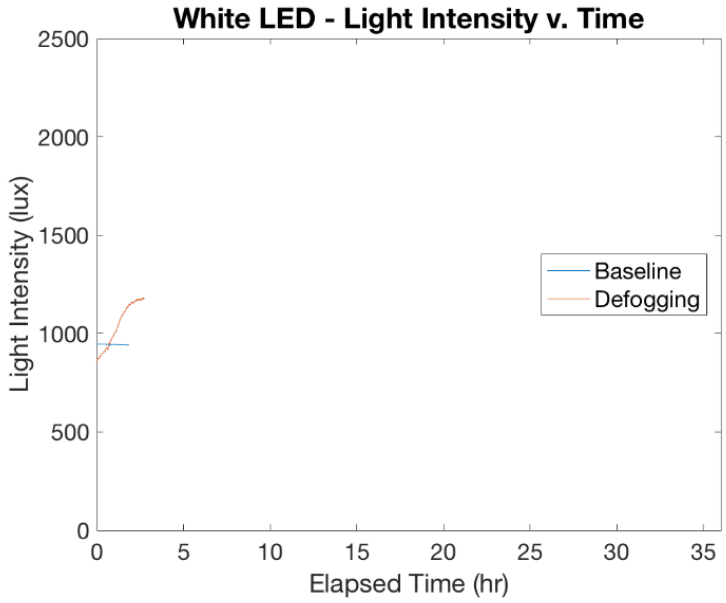

Figure 13. Another sample case of OMS testing with white LED leading to hardware failure, where the unknown failure terminated data acquisition early at three hours.

Figure 13 is also the most successful data acqusition session with the white LED, where PVT recovery is at least visible. Baseline light intensty measurements in Figure 13 showed a steady plateau at an average value of 944 ± 2 lux. The white LED baseline measurements showed the most stability of all the LED baseline data, but acquisition only lasted for a total of three hours before another OMS hardware failure. In comparison, the maxmimum value during PVT recovery was 1174 ± 5 lux before data acquisition failure. It is unknown if the light intensity would have plateaued at this lux value, but the beginnings of a plateau in measured light can be seen which indicated the light intensity was measured at or near to the point of PVT recovery.

Despite the consecutive failures, preliminary results indicated that white LED measured light would recover at a much faster rate than the measurements from blue or green LEDs. As the first OMS/LED tested in prototyping, it is hypothesized that white LED tests were conducted before the defogging effects in the freezer was discovered. Thus, testing with white LEDs likely occurred with partially transparent PVT samples and the overall recovery time was accelerated. Another hypothesis was that the scattering effects of water particles in fogging (synonymous to natural fogging) is less significant on the white LED light as the blue or green, thus the change in lux values may be less gradual and seem to indicate the PVT recovered faster.

The final range between minimum and maximum white LED light intensities was 321 lux, where the maximum light intensity exceeded the baseline value by a difference of 230 ± 5.4 lux (percent difference of 24.4%). The difference between light measured at

recovery and the baseline indicated that longer acquisition time may not have been necessary because the recovery data had already exceeded baseline.

Measurements from the red LED are seen in Figure 14 and showed the shortest recovery time and the smallest range of 111 lux between minimum and maximum light intensities. The baseline light intensity averaged at 379 ± 1 lux for two hours before OMS failure. The light intensity at PVT recovery averaged at 462 ± 1 lux. The final steady state from the red LED exceeded the average baseline by 83 lux, with a 21.9% difference between the two values. Despite the early termination of the baseline data acquisition, the large discrepancy indicated that a larger set of baseline data would not have contributed much to the comparison.

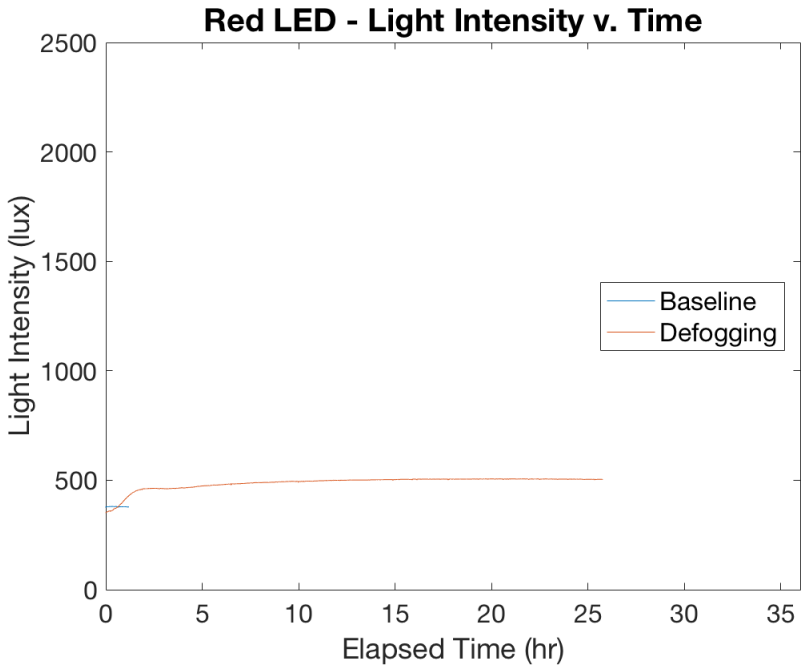

Figure 14. Light intensity from OMS testing with red LED. Light intensity increased asymptotically to a plateau that exceeded the baseline intensity measurements.

Table 3. Summary of light intensity measurements from Figure 6 comparing baseline measurements to the maximum light intensity at PVT recovery, and percent difference.

LED Color	Average Baseline Light Intensity (lux)	Final Recovery Light Intensity (lux)	Percent Difference
Green	920 ± 5	828 ± 2	-10.0%
Blue	2098 ± 13	2076 ± 1	-1.0%
White	944 ± 2	1174 ± 5	24.4%
Red	379 ± 1	462 ± 1	21.9%

Light intensity from the green LED also failed to recover to the original baseline measurement, seen in Table 3. Maximum lux fell short of the baseline by an average of 92 lux. From the prototype testing, the relationship of light intensity measurements from baseline values and PVT recovery process varied greatly. Some of what is seen may be attributed to the scattering effects of fogging on perceived light, which becomes more significant with increasing wavelength. Ideally, the baseline values were to establish a means of comparison, where light intensity measured at full PVT transparency was supposed to match before fogging and after recovery.

All attempts to replicate these discrepancies were unsuccessful. At times the light intensity at recovery failed to match the baseline average; while at other times the intensity at recover far exceeded the baseline average. Discrepancies changed between data acquisition session and LED color. Light intensity behavior was never repeatable between two recovery sessions involving the same LED.

Regardless, results from the prototype testing were considered successful. The expected trend of increasing light intensity as PVT recovered was clearly observed in all data capture sessions. The COTS hardware was capable of emitting light and detecting light through the thickness of the PVT plastic. Light intensities were seen beginning at a minimum value when the PVT was fully opaque and an increase in lux was seen as the detector recovered. These trends show that a rate of change is distinguishable across all LED colors. Functionality of the OMS was thus demonstrated and showed that the measurement of light intensity was a success using COTS parts. The basic design of the OMS from prototyping was therefore retained and any further developments were focused on improving functionality and OMS construction.

CHAPTER IV

FINAL DESIGN

OMS Modifications

Design Evaluation

Results from the prototype testing led to additional design evaluations and revisions in preparation for final testing. One of the main issues was consistency between testing. While the basic design of the OMS was retained from the prototyping, it was determined that some improvements to the design's robustness be made to minimize the hardware failures seen during testing. All components in the OMS were re-soldered and joints reinforced with E6000 adhesive. The adhesive was applied to reduce water intrusion and prevent moisture uptake inside the wiring. It also provided a stiffening effect to fortify the soldered joints and resist detachment. Each joint was again shrink wrapped. A clear, silicone optical gel was also added to increase optical clarity between the LED and the lux sensor. The silicone gel was applied to the surface of the PVT plastic directly underneath the lux sensor and LEDs prior to encapsulation.

Consecutive LED failures occurred between data capture sessions; therefore, the OMS was outfitted with an array of LEDs instead of a single. The array specifically addressed the LED failures during recovery measurements. An array of LEDs would ensure the OMS continues to operate in the event of a single LED failure. The design addition involved an array of LEDs arranged in a line rather than a stacked bundle for two reasons: the array lies flat against the detector face and is more easily integrated into RPM enclosures. Malfunctions in LEDs were unnoticeable during the soaking and

freezing period and only revealed during recovery testing. Therefore, an array of LEDs would ensure the OMS operations continue if a single or even multiple LEDs failed. The array consisted of red, green, blue, white, and yellow LEDs packaged together with separation maintained by a stacking header, seen in Figure 15. Additional LEDs of varying colors also allowed for more streamlined testing, where light intensity measurements for all colored LEDs can be gathered within one recovery test.

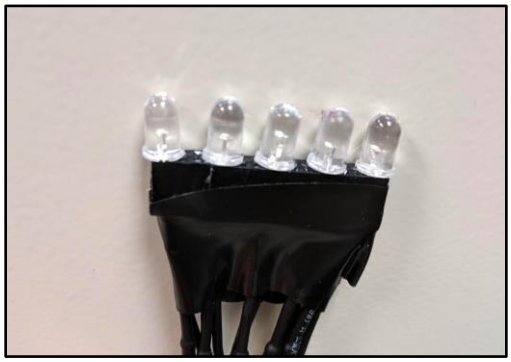

Figure 15. The LED array consisting of red, green, blue, white, and yellow LEDs, which replaced the single LED design in the OMS.

Each LED in the array was separately prepared with E5000 and shrink wrapping. Power and data transmission were separated by routing the LEDs through different digital output pins on the microcontroller. The array was attached to the detector face with the center LED aligning with the center of the lux sensor. Securing the array to the detector face with electrical tape was required prior to wrapping due to the array shifting and sliding while wrapping the detector in foil.

Some final testing was conducted utilizing the laboratory environmental chamber and prototype procedure. Following initial tests, it was seen that the PVT plastic fails to

return to full transparency despite recovering to RT at RH. This was expected given the fogging effect is a result of microfractures within the plastic, which are exacerbated by environmental extremes. To ensure each PVT began at full transparency, the detectors were a subjected to 24-hour high heat session in the environmental chamber. This was achieved by removing the water from the ice chest and allowing the prepared PVT detectors to sit with the heat lamp on for 24 hours. To confirm full transparency was achieved, the control PVT detector without wrapping was used. The heated 'bake' was integrated into the environmental measurement procedure after each recovery test and before each soaking and freezing session. This modification in heating and freezing procedure was integrated during the final few data capture sessions.

Data Capture Sequence

The design change from a single LED to an LED array required additional actions in the data capture sequence. Single digital output pins per LED ensured each LED flashed individually, allowing for specific on-off sequencing along the array. Color coded wires for specific functions was carried over from the prototype design and was essential in maintaining organization when constructing the LED array. Final design layout of the OMS is illustrated in Figure 16, which shows the location of the pins for each component of the system onboard the microcontroller. A description of the pin function, color-coding key of the wiring, and the pin location on the microcontroller can be found in **Error! Reference source not found.**.

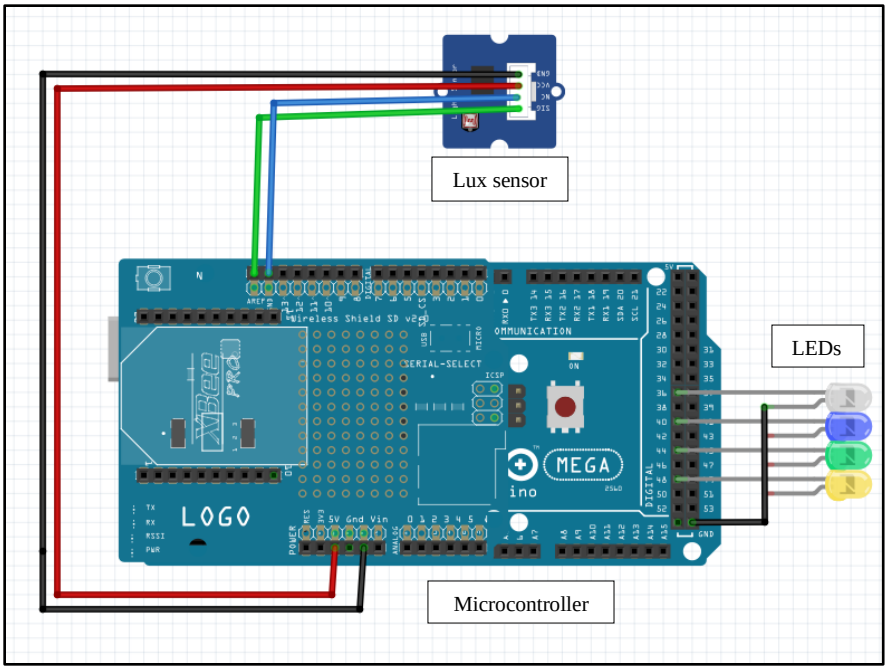

Figure 16. OMS components and associated pinout on the Arduino Mega microcontroller. Refer to Table 4 for description of component and wire color.

Table 4. OMS components and associated pinout on the Arduino Mega microcontroller seen on the final design. Design illustration can be seen in Figure 16.

Component	Wire Color	Arduino Pin
OS SCL	Green	SCL
OS SDA	Blue	SDA
OS Voltage In (Vin)	Red	5 V
OS Ground (GND)	Black	Ground
LED Positive (+) Wire	Gray	White: Digital Pin 36 Blue: Digital Pin 40 Green: Digital Pin 44 Yellow: Digital Pin 48
LED Negative (-) Wire	Black	Ground

The design modification required each of the five LEDs to activate consecutively and a measurement was captured by the lux sensor 100 ns after an LED activation. The delay allowed the LED to reach full brightness before a measurement. This sequence repeated at 60 s intervals until the end of the data capture operation. Light measurements were again recorded in serial data format, which is captured by the Arduino mega microcontroller and recorded on the testing computer in CoolTerm. The final serial output showed a string of lux values where a comma separated each measurement, the sequence of light measurements corresponding with the sequence of LEDs. Order of the LEDs was important to note and was kept consistent between tests to ensure each readout on CoolTerm corresponded with the correct LED.

CHAPTER V

ENVIRONMENTAL CHAMBER TESTING

Full Scale Design

Following the prototyping stages, where the design of the OMS was proven functional and met the design criteria, the system was tested on ‘full-scale’ PVT detectors measuring 3.8 cm x 15.2 cm x 76.2 cm. As the standard size employed in RPMs, final testing required the 76.2 cm tall detectors to ensure the OMS design could carry over from the prototype stage. Given that functionality had been demonstrated with the OMS mounted on the smaller PVT, results from the 76.2 cm detectors would establish the final design. Small openings were created on the broad sides of the detector faces, enough to slip in the LED array and lux sensor. Each component was placed in the center of the detector face, careful to ensure the lux sensor and the LED array were properly aligned across the plastic. All OMS components received the same treatment of optical silicone gel and sealed in layers of electrical tape to preserve a tight seal on the detector face. Figure 17 shows the final appearance of the PVT detector and OMS. Silicon covered stranded wires were used in place of plastic covered wire to allow for flexibility and prevent wire breakage. Though the OMS components were to sit flush against the detector faces, a protruding band of electrical tape was added to relieve strain on the soldered joints of the lux sensor during testing. The sequences for data capture remained unchanged for the LED array and no further additions were made.

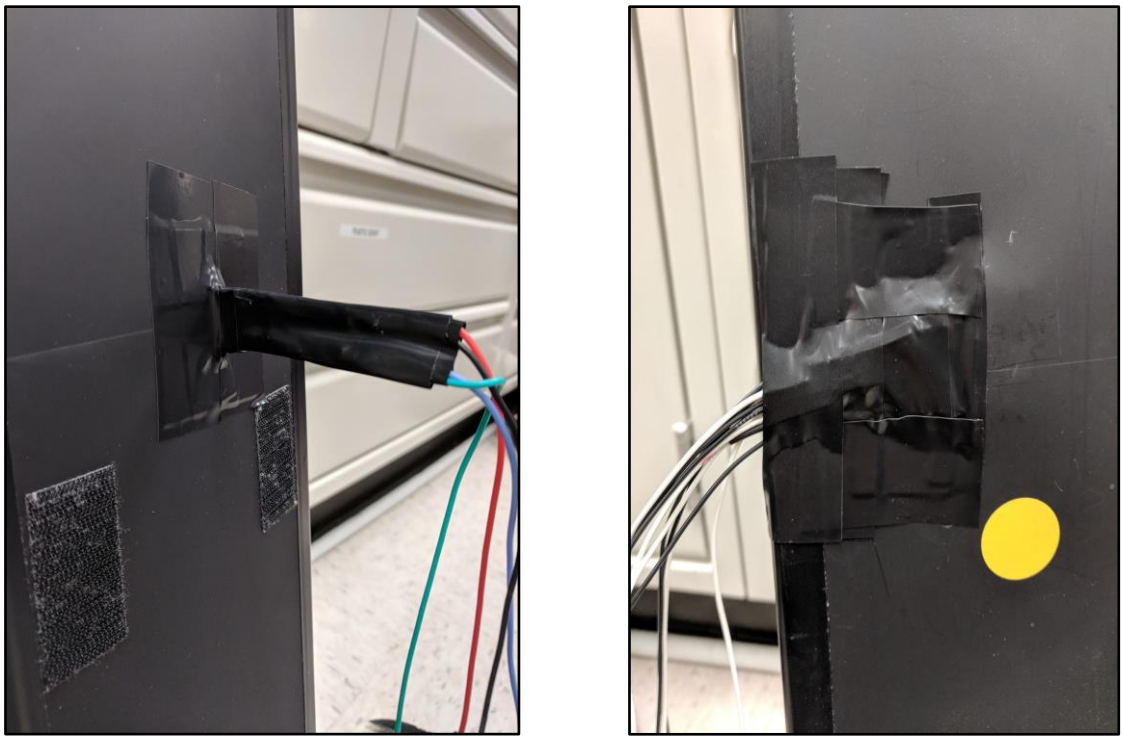

Figure 17. Final placement of the OMS components on the 3.8 cm x 15.2 cm x 76.2 cm PVT detectors PVT detector. Location of the lux sensor (left) and location of the LED array (right) on directly opposing faces of the PVT.

As the detectors came from the field pre-wrapped, it was determined that utilizing the professional wrappings would produce a better result than re-wrapping in the laboratory space. Given the larger detector size, the laboratory built environmental chamber and freezer were no longer suitable for testing. Instead, a single PVT detector was prepared with the OMS onboard and sent off to be tested in a full-scale environmental chamber at Oak Ridge National Laboratory in Knoxville, Tennessee. Accompanying the OMS and PVT were Arduino Mega microcontrollers and SD cards for data capture. The PVT became inaccessible in the environmental chamber; therefore, hardware troubleshooting was not possible. Special care was taken to ensure the OMS

components were still functional after shipping to Knoxville that included well insulating packaging and tape to minimize shifting of the detector during shipping.

Environmental Chamber Testing

Final testing of the OMS/PVT system was conducted at ORNL. This facility had a dedicated, large environmental chamber dedicated for NSDD research. Scientists at this facility also had an established procedure of exposing the crystal to promote fogging. Temperature and humidity data were acquired from an ORNL computer that was associated with the environmental chamber. The serial data was transferred to Texas A&M University for analysis after the environmental chamber test. This data and the corresponding output from the OMS were paired together manually. It should be noted that as a result of data collection through two different systems, the time alignment of the data is not perfectly matched. It is believed that the differentiation between data sets does not influence the conclusions of this research.

Cycling Procedure

Beginning with initial RT and RH at 20℃ and 40% respectively, the PVT/OMS system was were subjected following temperature and humidity changes. To ‘season’ the PVT detectors by opening the microfissures in preparation for water uptake, the temperature was raised to 55℃ at 100% RH with a rate of 10℃ hr^{-1} and was maintained for eight hours followed by a return to RT and RH at a rate of -5℃ hr^{-1}. The chamber increased to 55℃ at 100% RH for 170 hours to induce water uptake into the PVT detector before returning to RT and RH. Data captured during the 170-hour soak established the baseline light intensities for each colored LED. The change in LED light

perceived was compared throughout each of the temperature cycles to establish if a distinct reduction can be seen while the PVT fogged and recovered.

The following cycles were repeated for a total of 888 hours to depict fogging and recovery of the PVT detector: high humidity and high temperature soak at 55℃ for six hours, then cooled over twelve hours to -20℃ at a rate of -10℃ hr^{-1} followed by heating back to 55℃ at the same rate of -10℃ hr^{-1} over twelve hours. Individual heating and cooling cycles took 30 hours. Between operational time of approximately 560 hours to 650 hours, the environmental chamber experienced a facility-wide power outage and caused temperatures to stabilize at 22.5℃ and unknown humidity. Temperature values taken from the thermocouple can be seen in Figure 18 and include the 170-heat soak plateau and the facility power loss plateau.

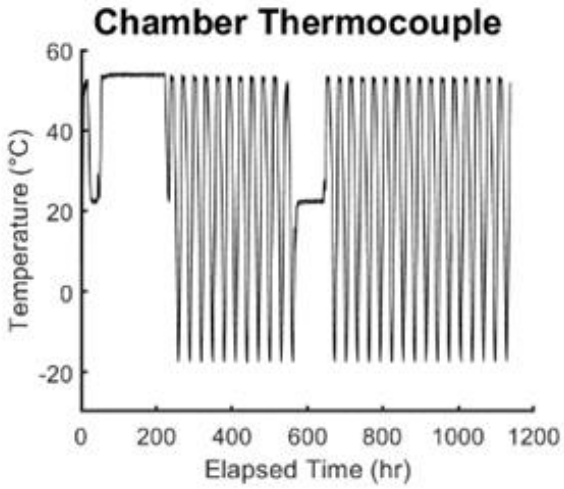

Figure 18. Temperature values from the environmental chamber throughout testing at ORNL. The plateau at 22.5C between the operationl hours of 560 to 650 was due to a facility-wide power outage.

Data Capture Results

Baseline Values and Observations across all LED Colors

The PVT detectors within the environmental chamber were confirmed to have fogged through visual inspection of the PVT through a window cut into the detector wrapping. The PVT plastic can be seen in Figure 19 where full transparency is observed prior to environmental chamber testing. Severe and lasting damage was then seen in the same detector after the 1000 hours, such that the plastic remains opaque even at RT. The fully unwrapped PVT detector following testing can be seen in Figure 20.

(A) (B)

Figure 19. Sample of PVT detector before environmental chamber testing (A), and the same sample after 1000 hours of cycling temperature and humidity (B) where the sample was severely damaged and remained opaque at room temperature.

Examination of the test PVT showed that the plastic detector suffered significant damage due to the microfractures caused by temperature extremes and was unable to recover to transparency at RT and RH. This emphasizes the importance of opacity

tracking for PVT detectors, whereby degradation must be monitored to ensure maximum functionality for existing RPM systems that utilize these detectors.

Figure 20. The PVT detector remained fully opaque at room temperature and RH as a result of significant damage from microfractures following multiple temperature cycles in the ORNL environmental chamber.

Light intensity values obtained during OMS testing are seen in Figure 21 organized by LED color as a function of time, and some observations can be made that apply to all color datasets. Environmental chamber temperature as a function of time can also be seen in Figure 21. Initial comparisons show that the white LED dataset varied to a degree that was not seen in the other LEDs. Regardless, general observations of the datasets show that a difference can be seen between the minimum lux value and a maximum lux value. This result is promising as it indicates that discernable changes in perceived light across the PVT can be detected with the OMS. Further analysis for the blue LED, green LED, and yellow LED datasets will be discussed individually.

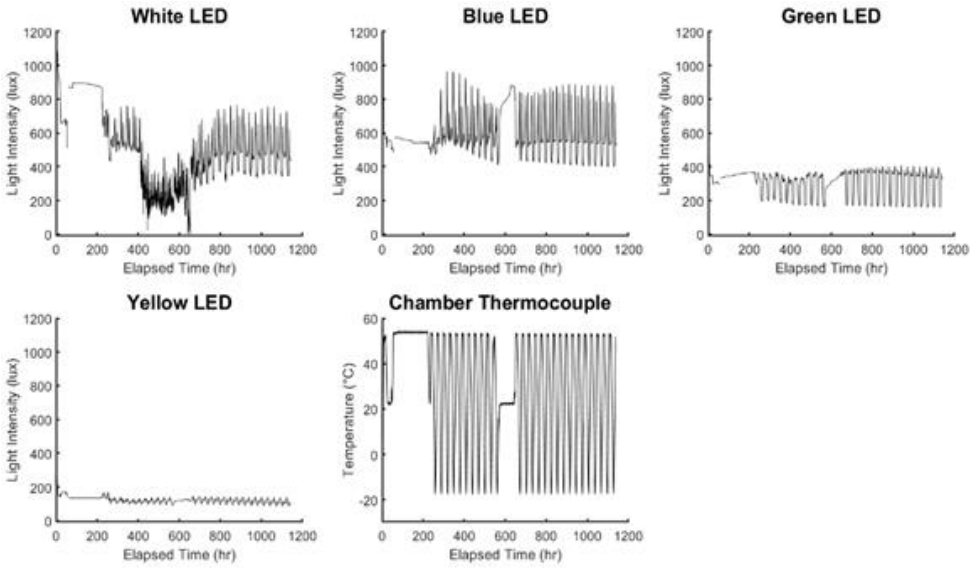

Figure 21. Light intensity values from OMS testing at ORNL as a function of operational time. Environmental chamber temperature as taken from a thermocouple as a function of operational time is also shown.

Analysis of the dataset begins where a 170-hour long heat soaking occurred at 55°C and 100% RH. A stable light intensity was expected given the consistent temperature and PVT transparency during this period, given the temperature cycling had not been initiated at this point of the test. Light measured from the green LED increased over the 170 hours while blue and white LED light decreased. Yellow LED light measured the most consistency during the heat soak. A comparison of the initial lux taken at hour 85.56 of the 170-hour soak and a final lux measured at hour 223.3 is summarized in Table 5. These values were taken not at the initial and final time of the 170-hour soaking, but where the light intensity measurements plateau and a ±1 lux change was seen. An average was taken between the initial and final values as well.

Table 5. Comparison of lux values at the start and the end of the 170-hour soaking period. Initial lux value was taken at hour 85.56 and final lux value was taken at hour 223.3.

LED	Initial Value (lux)	Final Value (lux)	Percent Difference	Average Value 'Baseline' (lux)
Blue	570	543	-4.73%	556.50 ± 13.50
White	891	870	-2.36%	886.40 ± 10.17
Green	336	364	8.33%	353.10 ± 10.06
Yellow	135	139	1.48%	135.01 ± 0.28

Quantitatively, the highest percent difference between lux values from the beginning and end of the 170-hour soaking period was seen in the green LED dataset at 8.33% and confirms what was observed in Figure 21. The decreasing change in the blue and white LED datasets were a difference of 5.79% and 2.36% respectively. Thus, the light intensity measured during the 170-hour soak were considered acceptable as baseline values for each LED and were thus used to compare the rest of the datasets. Analysis of these values showed that light change in the 170-hour-plateau were all within a 2σ variance for each average. Thus, the average lux calculated for each LED light was also used as the baseline for each LED dataset.

Power Failure Plateau

A second plateau observed in the datasets (see Figure 21) occurred between 560 hours and 650 hours and was due to a power outage that brought the environmental chamber to a constant 22.5℃. The light intensities were expected to correspond with temperature readings and plateau as well, given the unchanging temperature and

consistent PVT opacity. However, all LED datasets showed that the light measured increased during the power failure instead.

The shape of the transmitted light data for each LED was observed to change at different rates, each unique to the LED. This effect is hypothesized to be synonymous fogging effects on light of different wavelengths in nature. Further discussion on the phenomenon will be presented, as similar effects on the measured light is seen again when the datasets are analyzed. All LED lights showed an increase over time, and a linear fit calculation was conducted to determine the rate of lux change over time. The fit was taken where the shape of the slope was most linear. The blue light increased at a rate of 1.99 ± 0.009 lux/hr and the green LED increased at a rate of 0.0283 ± 7.10E-5 lux/hr. The yellow LED light also increased, but at a rate of 0.18 ± 7.32E-4 lux/hr. The white LED suffered a hardware failure that continued throughout the power outage and showed no distinguishing trend.

Analysis of the lux change lead to the hypothesis that the PVT detector may have been increasing in temperature throughout the power failure. The increases in light measured may be reflecting the slow return to transparency over time. The difference in rates between the LEDs is again similar to the rates of change seen during prototyping baseline measurements, the lux change over time was the largest in the blue LED, followed by green LED and finally yellow LED. The difference from LED to LED is again theorized to be the result of light scattering in the presence of fog synonymous to light interaction with natural fog. Light scatters more readily with shorter wavelength, thus the blue LED light may be more dispersed across the plastic before reaching the lux

sensor. Green LED light is the next shortest wavelength which also exhibited some of the scattering characteristics but not as strongly as the blue LED. Yellow LED and red LED have the next longest wavelengths after green; thus, the least scattering may be seen.

Overall, discernable differences between high and low temperatures could be seen through the OMS design with all colored LEDs. Closer inspection of the light intensity peaks and temperature was made to determine any correlation between the two. Figure 22 shows the dataset from two temperature cycles. The lowest light intensities appear to align with the low temperatures of the cycles, and the highest light intensities correlated with 55°C point of each cycle. The functionality of the OMS was thus demonstrated as the measured lux values indicate diminished opacity changes in the PVT detector over time as a function of temperature variations. Further analysis of the dataset was required to determine the relationship between OMS output and the opacity change within PVT.

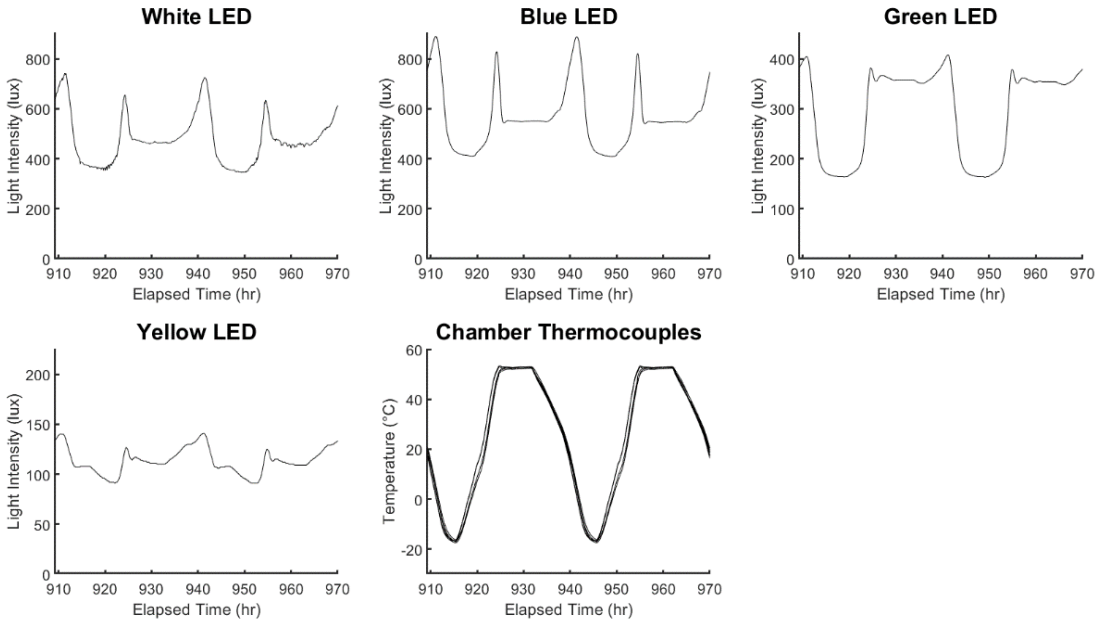

Figure 22. Isolation of two temperature cycles, showing light intensities as a function of time for white, blue, green, and yellow LED datasets with the associated thermocouple data.

Analysis of a single temperature cycle showed a distinct three-region characteristic could be identified in the light intensity cycle. These regions began with a lux minimum that increased to a localized peak, a decrease in lux that plateaus, then another increase that peaks to an absolute maximum light intensity (higher than the first localized maxima) before decreasing to an absolute minimum. These characteristics then repeat with each temperature cycle. For the purpose of discussion, the three characteristic regions were named: the rise to a local maximum (RLM) region, the plateau region, and the trench region, respectively. Location of the three regions over one light intensity cycle is illustrated in an example Figure 23. The example figure segments the data into the aforementioned regions using the dataset label ‘Blue’,

however it should be noted that not all the regions in Figure 23 align, as the case with the ‘Green’ dataset, or is less distinguished such as in the ‘Yellow’ dataset.

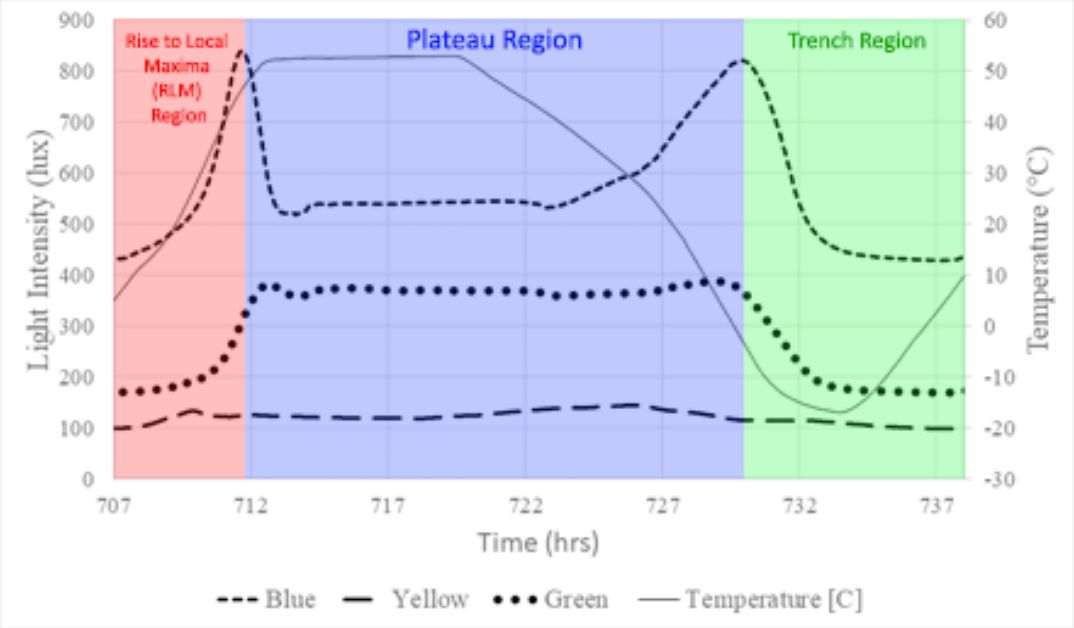

Figure 23. Light intensity and temperature data over one temperature cycle with three distinct regions identified in the light intensity; the RLM region where lux rises to a local maxima, the plateau region where lux drops to a steady plateau then rises again, and the trench region where lux peaks at an absolute maxima then falls to an absolute minimum.

Beginning in the RLM region, OMS light intensity first peaked where the environmental chamber temperature was on the rise towards 55℃. The environmental chamber did not reach the maximum 55℃ until approximately 1 hr after the appearance of the local maximum. When chamber temperature did reach 55℃, light intensity measured from all LEDs had transitioned into the plateau region where lux decreases then reaches a steady state. The measured light then stays in the plateau region while the chamber is held at 55℃. This was an unexpected feature given that the OMS should

theoretically reflect PVT opacity, and PVT opacity is known to remain steady to reflect a steady temperature ((Lance M. J., 2019). The chamber temperature begins to decrease from 55℃ while the light intensity is midway through the plateau region. Chamber temperature continues to decrease but light intensity beings to increase and peaks again for an absolute maximum and the beginning of the trench region. The peak is considered an absolute maximum as it is consistently higher of the local maximum (located in the RLM region). Only after the absolute maximum does the lux intensity decrease while the temperature is also decreasing before finally reaching a minimal light intensity.

This trend in lux data was repeated for all LED colors across all temperature cycles until the end of the environmental chamber test. This three-region behavior is contrary to what was expected. Prior to the environmental chamber test, it was assumed that OMS light intensity directly correlated with the state of PVT opacity in a cyclic nature, which is known to be associated with temperature cycles. Therefore, diminishing measured light would align with temperature decrease (from RT) then followed by increase in measured light when temperatures increased. Likewise, the OMS should record the lowest of light readings when temperatures reached a minimum and the brightest light measured when temperatures reach a maximum.

Aside from the three region characteristics, the behavior of OMS light intensity reflects changing temperature, but on a slightly delayed time scale. Where the temperature stabilizes, it could be seen that the light intensity will also stabilize after some time delay. This delay is likely the result of a temperature difference between the PVT detector and the temperatures reported by the thermocouple which reflects the

temperature of the environmental chamber. Composed of insulating plastic, the internal temperature PVT detector will increase at a slower rate than the environmental chamber. Light intensity reported by the OMS is the opacity of the detector plastic at the time and is directly affected by internal temperature of the PVT rather than the thermocouple reading.

Analysis show that the fogging effects on light of varying wavelengths is most visible in the blue LED and green LED datasets. The blue LED light maxima in the RLM regions that are approximately 1.5 larger than the light measured during the heat plateau. Blue wavelength is the shortest at approximately 430 nm and thus scattering effects are more pronounced. Scattering effects are likewise shown to increase with increasing wavelength. Green LED, with the second shortest wavelength of approximately 560 nm demonstrated the next largest local maxima, followed by yellow LED (with a 590 nm wavelength). Similar effects are seen in light intensities with decreasing temperatures following the 55ºC heat cycle. Again, it is theorized that water condenses within the microstructures developed in PVT which allow scattering to dominate and in turn increasing the intensity of observed light. While temperature continue to decrease, PVT fogging increases and absorption dominates which decreases light intensity until a minimum is seen. Additional tests must be performed for verification.

Relating PVT Opacity and Light Intensity

Establishing a correlation between the environmental chamber temperature and OMS light intensities is crucial to understanding OMS output for tracking the onset fogging in the PVT plastic. Due to the strong correlation between temperature and PVT opacity, a change in opacity may be deduced by quantifying any light reduction between high temperature states and low temperature states. Low light intensities were shown in the dataset (found within the trench regions) and high light intensities were recorded during the 55 ℃ heat-plateau of each cycle. An Opacity Ratio (OR) was established for each LED dataset and compares the average minimum light intensity to the average light intensity in the heat-plateau's, seen in Eq. 1.

$$\boldsymbol{Opacity\ Ratio\ (OR)} = \frac{\boldsymbol{Average\ lux\ at -22°C\ (minimum)}}{\boldsymbol{Averaged\ lux\ at\ 55°C\ (maximum)}} \qquad \textbf{(Eq. 1)}$$

For the purpose of comparison, an average light intensity was determined when the PVT was at equilibrium temperature with the environmental chamber. These values shall be discussed by LED color, as follows. Ideally, a small OR should be seen which would reflect the large difference between light intensity at high and low temperatures. To precisely track opacity changes in the PVT detector, a large range between high and low light intensity is preferred. Results were expected to show a difference between light intensity measured at maximum and minimum temperature. The difference should be distinguishable so that the onset opacity changes within the PVT plastic is easily identified.

Blue LED

The blue LED dataset showed that the light measured over each temperature cycle differed before and after the chamber facility power failure (seen in Figure 24). The shape of the measured light began to shift towards lower lux ranges with each cycle prior to the power outage but following the power failure the shape of the cycles was more uniform and repetitive.

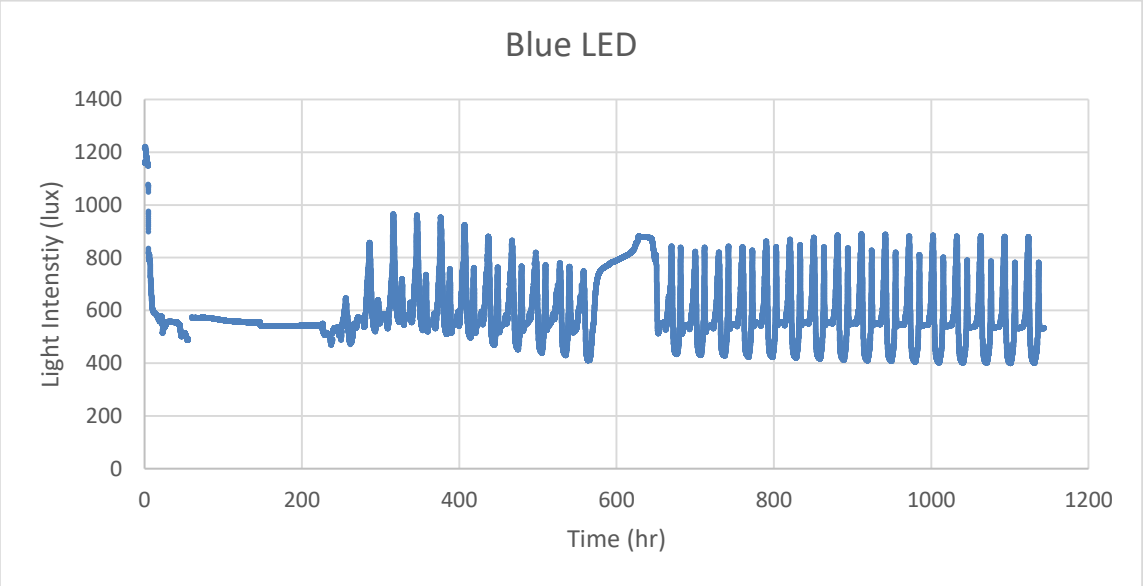

Figure 24. Light intensity measurements from the OMS with the blue LED.

Overall, light measured in the 55°C heat plateau averaged 551 ± 11 lux while the minimum light measured averaged 444 ± 44 lux. The error seen in the averaged minimums is a result of the cycles prior to the power failure, a feature that is also seen in the green and yellow datasets. The calculated OR for blue LED between the two values measured 0.81 ± 0.08, indicating that nearly a 20% reduction was seen between the absolute maximum peak and lowest light measured (at low temperature). Despite the

error seen in the minimum measured light, the OMS recorded a statistically lower values in transmitted light while tracking the onset fogging in the PVT plastic utilizing the blue LED.

Green LED

The cycles of light measured from the green LED became more uniform after the facility power failure, seen in Figure 25. Initial observations of the light cycle shapes showed that each cycle peaked at a different lux value before the power failure, while the peaks of each cycle after the power failure was more repetitive. This behavior is also similar to the shape of the blue LED cycles but the minimal of each green LED peaked more uniformly cycle to cycle after the power failure. Quantitative analysis for the green LED was conducted to verify or negate these observations.

For the green LED the average measured light in the 55°C heat plateau was 353 ± 13 lux while the average minimum light was 172 ± 12 lux. As such, the spread of the average minimal lux was 7% while the spread of the average light at 55°C was 4%. The values confirm initial observations that the minimum peaks of each light cycle are more consistent in the green LED cycles than the blue LED cycles.

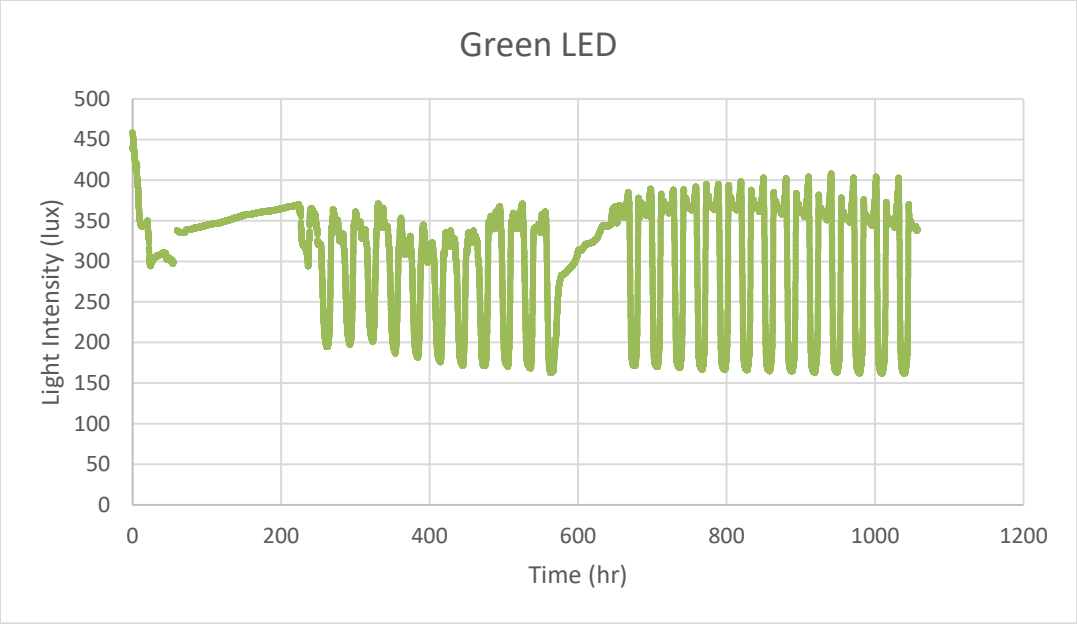

Figure 25. Light intensity measurements from the OMS of the green LED taken during PVT detector testing in an environmental chamber at ORNL.

Comparing the green and blue datasets show that some irregularity in the hardware function likely occurred in the cycles prior to the facility power failure, leading to light cycles that varied in shaped in both the blue LED and the green LED. The OR of the green LED was determined to be 0.49 ± 0.04. At nearly 50% reduction in light intensity, the OMS demonstrated even greater effectiveness at tracking opacity changes in PVT through the green LED.

Yellow LED

The light intensity measured from the yellow LED remained between 90 lux to 150 lux throughout the course of environmental chamber testing. The lux cycles were the least distinguished in the yellow LED dataset, which can be seen in Figure 26.

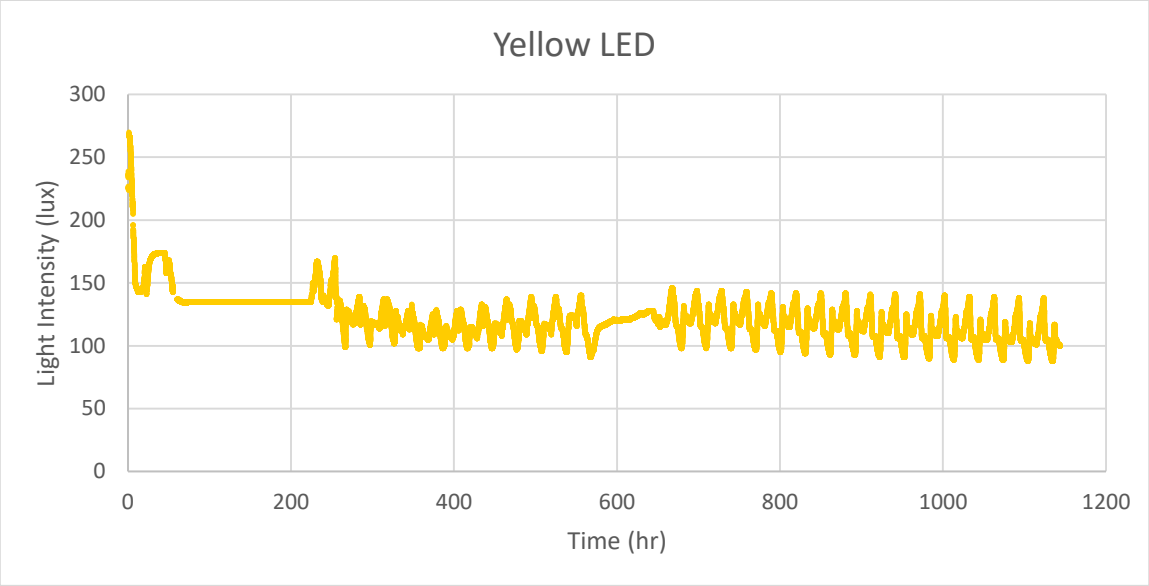

Figure 26. Light intensity measurements from the oms of the yellow LED taken during PVT detector testing in an environmental chamber at ORNL.

Comparison of the yellow LED to the blue and the green LED showed that the shape of each light cycle prior to the facility power failure seemed peak at a different maximum lux. Following the power failure, the shape of the cycles began to peak at similar maximums cycle to cycle. The cycle shapes seemed to reach a similar minimum peak prior to the power failure, but after the power failure each cycle seemed to reach a lower and lower minimum. The three-region characteristic is the least distinct across the yellow LED lux cycles such that light intensity appears to more closely correspond with rising and falling temperature. Average light intensity measured in the 55°C heat plateau was 114 ± 5 lux while the average minimum light measured was 95 ± 4 lux. As such, the OR for the yellow LED measured 0.84 ± 0.05 for a total of 16% light reduction between light intensity at high temperatures and light intensity at low temperatures.

White LED

Light intensity measured with the white LED showed significant variance throughout the environmental chamber test. During the 170-hour soaking period, the fluctuations in lux indicated a hardware malfunction occurred that affected light intensity measurements for the remainder of the test. The complete white dataset can be seen in Figure 27, where it is clear that almost no distinguishable cycling could be seen in the light intensity, particularly in the time leading up to the facility power failure.

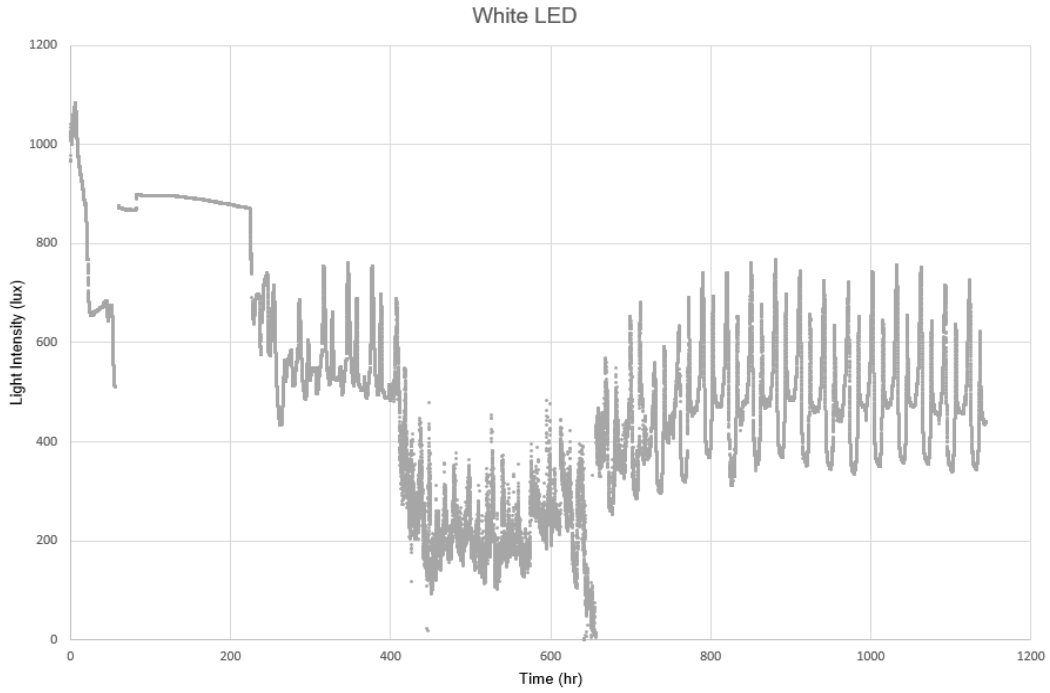

Figure 27. Light intensity measurements from the white LED of the OMS.

During the facility power failure, white LED light oscillated heavily and did not resemble the behavior of any other LEDs within the array. Given the inaccessibility of the OMS during testing, the malfunction was not identified until the data was analyzed.

The white LED malfunction appeared to correct itself approximately five cycles after the facility-wide power outage and a repeating pattern emerged in the cycles.

Initial observations showed that the widest range between light intensity at high temperature and low temperature could potentially be seen in white LED dataset. However, due to the reoccurring failures throughout the testing of the OMS, reliability of the white LED is questionable and average lux at 55°C and -22°C could not be determined with high confidence. Thus, the white LED was not recommended in the final design of the OMS array. However, the white LED data did demonstrate the validity of an LED array design. The hardware failure of the white LED was isolated and did not affect the performance of the other LEDs within the array, thus an array of LEDs is recommended for the OMS design over the single LED configuration.

Light Intensity in Summary

Overall, the OMS operated reliably with signs of a hardware malfunction but subsequently recovered and continued to provide reliable data in the form of measurable light. PVT opacity changes were clearly realized with high consistency throughout multiple hours of temperature cycling. A summary of the average light intensity at high and low temperature regions are seen in Table 6.

Table 6. A summary of the light intensities measured at high and low temperatures and the Opacity Ratio for blue, green, and yellow LEDs.

LED Color	Average Minimal Light Intensity (lux)	Average Light Intensity at 55°C (lux)	Opacity Ratio
Blue	444 ± 44	551 ± 11	0.81 ± 0.08
Green	172 ± 12	353 ± 13	0.49 ± 0.04
Yellow	95 ± 4	114 ± 5	0.84 ± 0.05

The OR of blue LED and yellow LED measured 19% and 16% reduction in light intensity respectively, while green LED showed a nearly 50% reduction. From the OR values, it was concluded that the green LED showed largest reduction in light intensity between at 55°C and the lowest lux values. This suggests that onset PVT fogging is most apparent through green LED light measurements. Therefore, the green LED is recommended for final design implementation of the OMS, followed by blue LED and finally yellow LED.

Isolated LED Testing Results

Following analysis of the OMS dataset from 1000 hours of cycling temperature and humidity, further testing was proposed to determine any effects of the environmental changes to the OMS's LEDs. As an integral component to the OMS system and composed of plastic, any effects on the LED's integrity from the extreme environment needed to be made known. Testing was conducted to address these concerns by examining OMS output in an environmental chamber without the presence of PVT.

Testing Procedure

LED testing was done by mounting the OMS on a wooden block with dimensions of 5.08 cm x 10.16 cm x 10.16 cm. The wooden block acted as a PVT plastic surrogate and ensured that data collected from the OMS was solely temperature independent of the PVT. Standard practices for mounting the OMS was conducted where the LED and OS were placed on opposite faces of the wooden block, centered over a hole cut into the block that separated the two components by 5.08 cm of air. The wood-

OMS system was wrapped in single layer of electrical tape and placed in an environmental chamber at 20 ºC and RH. Temperature was then increased to 50 ± 2 ºC at a rate of 5 ºC every hour. Light intensity measurements were taken every 60 s during the test. Following the 50 ºC peak, the environmental chamber was decreased to -22 ± 2 ºC at a rate of 5 ºC every hour. RH was maintained throughout the test.

For analysis, the results of the LED-wood tests were normalized to the light intensity measured at 50 ºC and can be seen in Figure 28. An average was found for each normalized light intensity and the results summarized in Table 7.

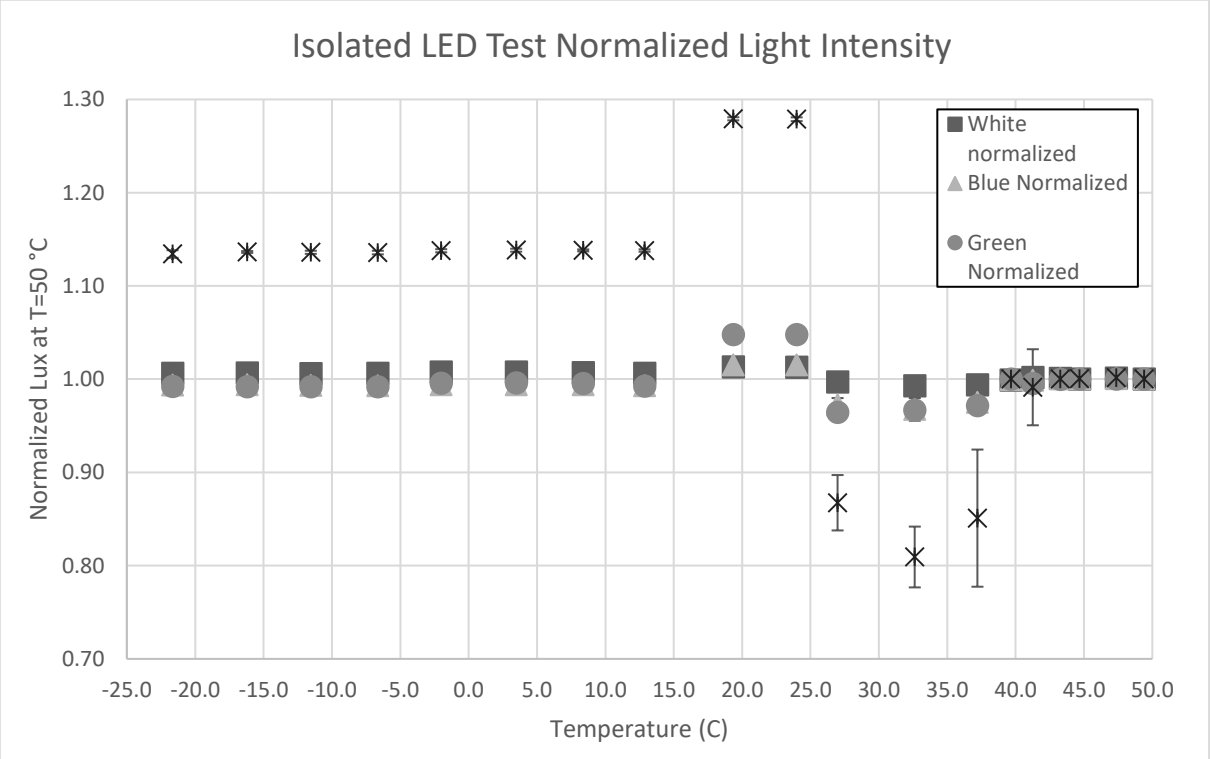

Figure 28. Light intensity results from the LED testing where the LED and OS were separated by 5.08 cm of air. Data is normalized to light intensity measured at 50 ºC with 1σ uncertainty.

Table 7. Average light intensity measured during LED isolated testing, normalized to the light intensity measured at 50 ºC for each color.

Color	Normalized Light Intensity	Maximum Ratio	Minimum Ratio
White	1.00 ± 0.01	1.01	0.99
Blue	0.99 ± 0.01	1.02	0.97
Green	1.00 ± 0.02	1.05	0.96
Yellow	1.06 ± 0.13	1.28	0.81

The normalized light intensity remained within 1σ across all LED colors except for the yellow LED which was within 2σ. These values in measured light intensities of the white, blue, and green LEDs. The yellow LED demonstrated the largest range of lux values and produced the brightest light at lowest temperatures. It was concluded that the OS and LEDs were not affected by the extreme temperatures based on the stability of the data throughout each temperature cycle. Thus, these results indicate that any light reduction seen at low temperatures are likely due to interference within the PVT plastic and not caused by reduced functionality of the OMS.

CHAPTER VI

CONCLUSIONS

In this research, a remote monitoring system known as an OMS was designed and tested. The system's purpose is to indicate presence of fogging within PVT by utilizing a measuring a difference in transmitted light through the plastic. The OMS design was developed in the laboratory and consisted of a lux sensor, an array of LEDs, and a microcontroller to encompass operational and data collecting functionality. A prototype was tested, and the design was modified in the laboratory setting before final testing for 1000 hours in an environmental chamber. Transmitted light was measured with the OMS and the data was subjected to analysis for determining the relationships between light intensity and PVT opacity change. Design evaluations and improvements were made following the analysis of the data

Analysis of the data obtained from the OMS during environmental chamber testing verified the design of the OMS which operated as intended. This conclusion was drawn from the fact that the OMS was capable of measuring light at a high temperature of 55ºC and extremely low temperatures and a difference was distinguished between the light at high temperature and low temperature. From the light measured, an Opacity Ratio (OR) was developed to quantify the observed change in light measured over the course of PVT opacity change. The OR determined are as follows: 0.81 ± 0.08 for the blue LED, 0.49 ± 0.04 for the green LED, and 0.84 ± 0.05 for the yellow LED. The reduction of light thus measured 19% for the blue LED, 49% for the green LED, and 16% for the yellow LED.

The OMS measured the brightest light at high temperatures utilizing the blue LED with an average of 551 ± 11, but the green LED demonstrated the largest overall reduction of 50% in light between temperature fluctuations. The importance of the LED array was shown, given an apparent hardware failure in a single LED that did not affect the outputs from other LEDs in the array. Reliability of the LEDs was also demonstrated in a series of tests without PVT plastic and light was measured consistently over the course of multiple cycles of extreme temperatures in an environmental chamber. The OMS design thus proved stable throughout multiple hours of operations and resistant to environmental extremes.

REFERENCES

Adafruit. (2013). *Adafruit Data Logger Shield*. Retrieved from learn.adafruit.com: http://learn.adafruit.com/adafruit-data-logger-shield/overview

Adafruit Industries. (n.d.). *Adafruit TSL2561 Digital Luminosity/Lux/Light Sensor Breakout*. Retrieved from adafruit.com: https://www.adafruit.com/product/439

Arduino. (2015, September). *Arduino Software (IDE)*. Retrieved from arduino.cc: http://arduino.cc/en/Main/FAQ#toc13

Byers, L. W. (2013). *Second Line of Defense Program Secondary Screening Field Data Collection--Summary*. DOE/LANL. doi:10.2172/1073744

Cameron, R. J. (2015). Fogging in Polyvinyl Toluene Scintillators. *IEEE Transactions on Nuclear Science , 62*(1), 368-371. doi:10.1109/TNS.2015.2390076

Fry, E. (1992). Coherent effects in forward scattering. *Ocean Optics XI. 1750.* San Diego: SPIE . doi:10.1117/12.140683

Janos, A. (2019, March). Root cause analysis and solutions for plastic gamma detector degradation in challenging environments—An overview. *Nuclear Instruments and Methods in Physics Research Section A: Accelerators, Spectrometers, Detectors and Associated Equipment*. doi:10.1016

Kouzes, R. (2004). Radiation Detection at Borders for Homeland Security. *American Physical Society, April Meeting.* Denver, Colorado: APS.

Lance. (2019). Nature of Moisture-Induced fogging defects in scintillator plastic. *Nuclear Inst. and Methods in Physics Research, A.*

Lance, M. J. (2019). Nature of Moisture-Induced Fogging Defects in Scintillator Plastic. *Nuclear Instruments and Methods in Physics Research Section A: Accelerators, Spectrometers, Detectors and Associated Equipment*. doi:10.1016/j.nima.2019.01.033

Meier, R. (2018, August 16). *CoolTerm*. Retrieved from freeware.themeiers.org: https://freeware.the-meiers.org/CoolTerm_ReadMe.txt.html

Payne, S. (2019, January). Predictive model of scintillator plastic fogging in portals. *Nuclear Instruments and Methods in Physics Research Section A: Accelerators, Spectrometers, Detectors and Associated Equipment*.

Science Direct. (n.d.). *Opacity* . Retrieved from https://www.sciencedirect.com/topics/chemistry/opacity

Singh, A. K. (2010). Opacity meter for transparency measurements. *5th IET International Conference on Power Electronics, Machines and Drives (PEMD 2010).* Brighton: IET. doi:10.1049/cp.2010.0114

Stuart, D. (2017, October 24). Opacity monitoring for measuring emissions. *25*(9).

Sword, E. D. (2017). Humidity-Induced Damage in Polyvinyl Toluene and Polystyrene Plastic Scintillator. *2017 IEEE International Symposium on Technologies for Homeland Security (HST).* Waltham, MA: IEEE. doi:10.1109/THS.2017.7943440

TAOS. (2018, July). *TSL,2561 Light-To-Digital-Converter*. Retrieved from adafruit.com/datasheets: https://cdn-shop.adafruit.com/datasheets/TSL2561.pdf

APPENDIX A

WHITE LED DATASHEET

SHENZHEN FURUIER PHOTOELECTRIC CO., LTD.

PRODUCTMODEL: FLR-50T04-HW7

LED Lamp

ØAbsolute Maximum Rating

Item	Symbol	Absolute Maximum Rating	Unit
Forward Current	I_F	20	mA
Peak Forward Current	I_{FP}	120	mA
Reverse Voltage	V_R	5	V
Power Dissipation	P_D	85	mW
Operation Temperature	Topr	-35~+80	℃
Storage Temperature	Tstg	-40~+80	℃
Lead Soldering Temperature	Tsol	Max.260° for 3sec Max.	

*I_{FP} Conditions:Pulse Width≤10msec duty≤1/10

*Tsol Conditions:4mm from the base of the epoxy bulb

ØTypicalOptical/ElectricalCharacteristics

Item	Symbol	Condition	Min.	Typ.	Max.	Unit
Forward Voltage	VF	IF=20mA	--	3.0	3.4	V
Reverse Current	IF	V_R=5V	--	--	10	uA
50% Power Angle	$2\theta_{1/2}$	IF=20mA	--	12	--	deg
Luminous Intensity	IV	IF=20mA	15000	20000	--	mcd
Chromaticity coordinates		IF=20mA	--	x=0.33 y=0.32	--	nm
Recommend Forward Current	I_F(rec)	--	--	10~20	--	mA

Notes:

1. Absolute maximum ratings Ta=25° C .
2. Tolerance of measurement of forward voltage±0.1V.
3. Tolerance of measurement of peak Wavelength±2.0nm.
4. Tolerance of measurement of luminous intensity±15%.

Add:Rd.HuaChang Nan.Tongfuyu Zone.Dalang.Longhua.Baoan District.Shenzhen.China.
Http://www.furuier.en.alibaba.com E-mail:ledexport@furuier.com Rev:A0 Page:2 of 5
Tel:86-755-61563456 Fax:86-755-61568736 Designed By:

ØPackage Dimensions And Materials

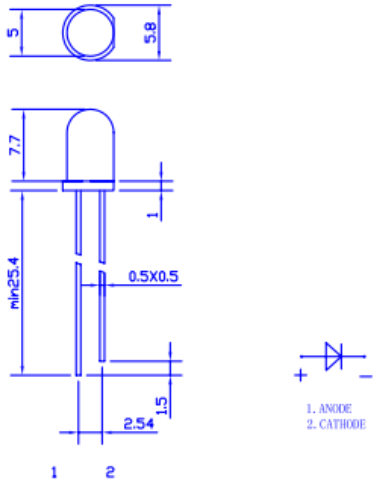

□ 0.5 SQUARE*2

Chip		Lens Color
Dice Material	Emitting Color	
InGaN	WHITE	WATER CLEAR

Notes:

1. All dimension units are millimeters
2. All dimension tolerance is ±0.2mm unless otherwise noted
3. An epoxy meniscus may extend about 1.5mm down the leads
4. Burr around bottom of epoxy may be 0.5mm max

ØSpatial Distribution

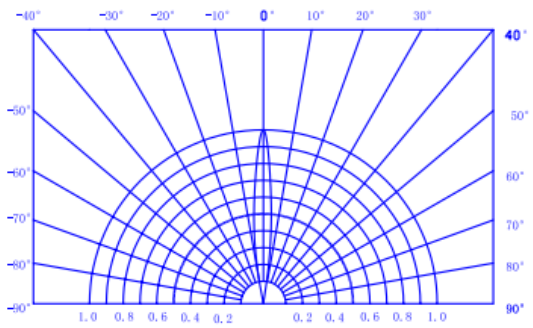

Rev lative Luminous Intensity Angle

ØReflow Temp/Time

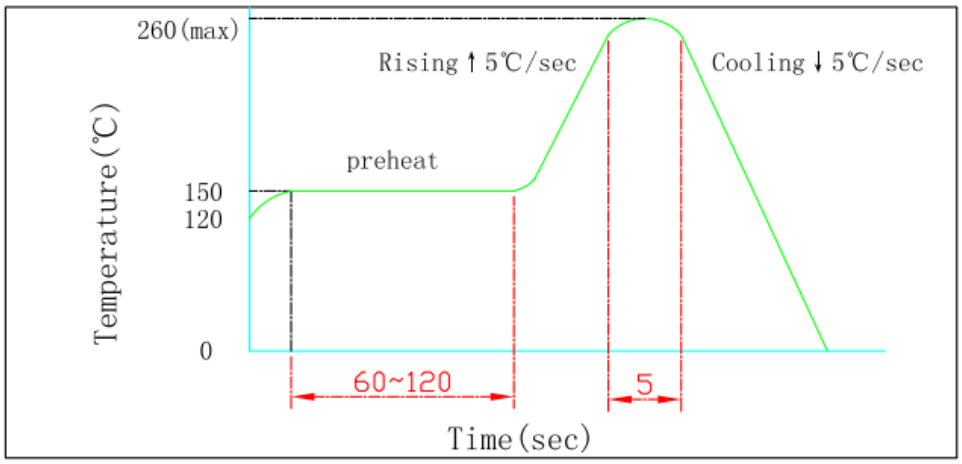

ØSoldering iron

Basic spec is≤5sec when 260℃. If temperature is higher, time should be shorter (+10℃-1sec) Power dissipation of iron should be smaller than 15W, and temperatures should be controllable. surface temperature of the device should be under 230℃

APPENDIX B

ELJEN TECHNOLOGY SILICONE GREASE EJ-550

SILICONE GREASE
EJ-550, EJ-552

EJ-550

These two materials are offered for use in optically coupling photosensors to scintillators and light guides. They are packaged in convenient squeeze tubes. Both have low bleed and evaporation rates at 25°C and are safe for handling and storage when exercising standard cleanliness procedures.

EJ-550 Optical Grade Silicone Grease is a clear and colorless optical coupling compound having moderate viscosity and providing excellent transmission properties well into the near-ultraviolet region. It should be stored at temperatures below 26°C, preferably below 5°C. EJ-550 retains clarity and fluid property down to -60°C.

EJ-552 General Purpose Silicone Grease is a translucent grease having high viscosity. It is recommended for use where the very best optical coupling is not required. It is best pressed out to a thickness below 0.1 mm where it becomes nearly transparent. It is best stored at room temperature.

PACKAGE SIZES	
EJ-550	EJ-552
450 g (1 lb jar) 150 g 90 g 30g	150 g

PROPERTIES	EJ-550	EJ-552
Specific Gravity	1.06	1.06
Refractive Index	1.46	1.47

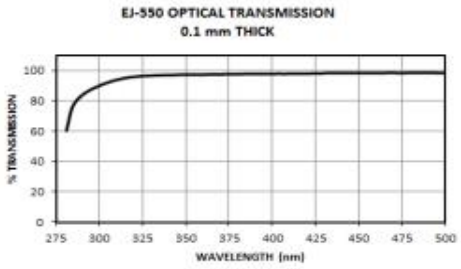

Revision Date: Aug 2019

ELJEN TECHNOLOGY
1300 W. Broadway, Sweetwater, TX 79556
www.eljentechnology.com • eljen@eljentechnology.com
Toll Free (USA): (888)-800-8771 • Tel: (325)-235-4276 • Fax: (325) 235-0701

APPENDIX C

MAGIC CHEF 6.9 CU. FT. CHEST FREEZER MODEL 3HMCF7W2 DIMENISONS

AND SPECFICATIONS

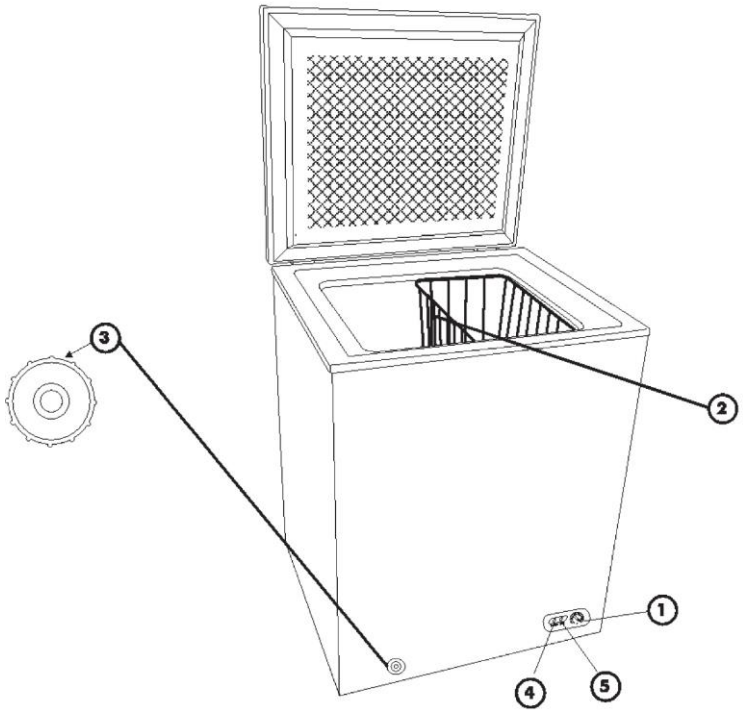

1. Temperature Control Adjustment
2. Vinyl Coated Wire Basket
3. Exterior Drain Dial
4. Power on Indicator (red)
5. Compressor on Indicator (green)

SPECIFICATIONS - MODEL # HMCF7W2

Product Description	Magic Chef Chest Freezer		
Model No.	HMCF7W2		
Capacity	6.9 Cu. Ft.		
Unit Dimensions	Width	Height	Depth
(inches)	36.9"	32.6"	22.0"
Net Weight (lbs)	79.4 (lbs)		